Science Advances
AAAS

advances.sciencemag.org/cgi/content/full/7/6/eabc6160/DC1

Supplementary Materials for

A GWAS in Latin Americans identifies novel face shape loci, implicating VPS13B and a Denisovan introgressed region in facial variation

Betty Bonfante, Pierre Faux, Nicolas Navarro, Javier Mendoza-Revilla, Morgane Dubied, Charlotte Montillot, Emma Wentworth, Lauriane Poloni, Ceferino Varón-González, Philip Jones, Ziyi Xiong, Macarena Fuentes-Guajardo, Sagnik Palmal, Juan Camilo Chacón-Duque, Malena Hurtado, Valeria Villegas, Vanessa Granja, Claudia Jaramillo, William Arias, Rodrigo Barquera, Paola Everardo-Martínez, Mirsha Sánchez-Quinto, Jorge Gómez-Valdés, Hugo Villamil-Ramírez, Caio C. Silva de Cerqueira, Tábita Hünemeier, Virginia Ramallo, Fan Liu, Seth M. Weinberg, John R. Shaffer, Evie Stergiakouli, Laurence J. Howe, Pirro G. Hysi, Timothy D. Spector, Rolando Gonzalez-José, Lavinia Schüler-Faccini, Maria-Cátira Bortolini, Victor Acuña-Alonzo, Samuel Canizales-Quinteros, Carla Gallo, Giovanni Poletti, Gabriel Bedoya, Francisco Rothhammer, Christel Thauvin-Robinet, Laurence Faivre, Caroline Costedoat, David Balding, Timothy Cox, Manfred Kayser, Laurence Duplomb, Binnaz Yalcin, Justin Cotney, Kaustubh Adhikari*, Andrés Ruiz-Linares*

*Corresponding author. Email: andresruiz@fudan.edu.cn (A.R.-L.); kaustubh.adhikari@open.ac.uk (K.A.)

Published 5 February 2021, *Sci. Adv.* **7**, eabc6160 (2021)
DOI: 10.1126/sciadv.abc6160

The PDF file includes:

Other Supplementary Material for this manuscript includes the following:

(available at advances.sciencemag.org/cgi/content/full/7/6/eabc6160/DC1)

Supplementary note: Regional association plots of the 23 regions detected here for which genome-wide significance association with non-pathological facial variation has been reported previously

Several of these regions are associated with multiple profile traits (See Fig. 2 of main text). Below we show plots only for the trait with strongest association to each region.

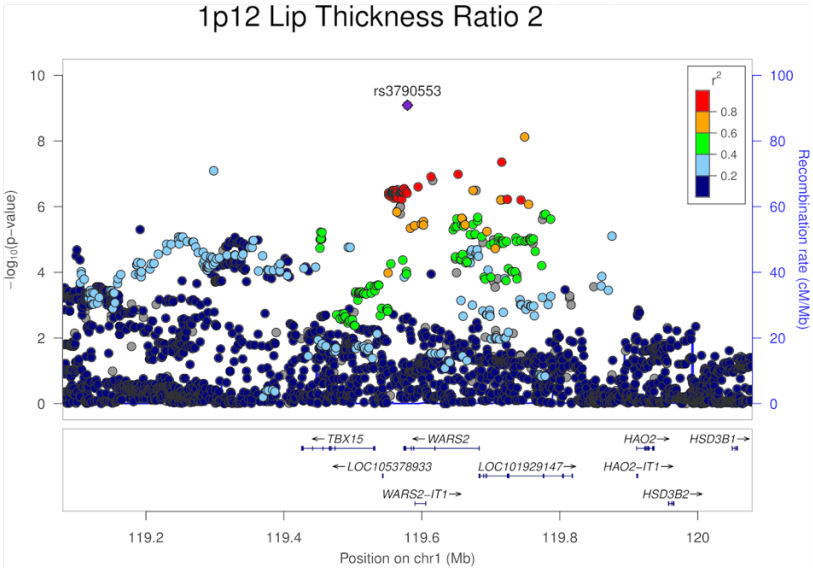

1p12: *WARS2, TBX15*. We associated SNPs from *WARS2* (tryptophanyl tRNA synthetase 2, mitochondrial) and *TBX15* (T-box transcription factor 15) region with traits related to lip thickness. This region was first associated with ear phenotypes *(15*). It has also been associated with the upper face area *(10)*, chin dimples *(7)* and mid-face morphology *(18).* Homozygous mutations in the TBX15 gene can induce Cousin syndrome (OMIM #260660). People with this condition presents particular facial phenotypes: frontal bossing, narrow palpebral fissures with deep set globes, hypertelorism, posteriorly rotated and low set ears. In mouse embryo, *Tbx15* is expressed in craniofacial region *(4).*

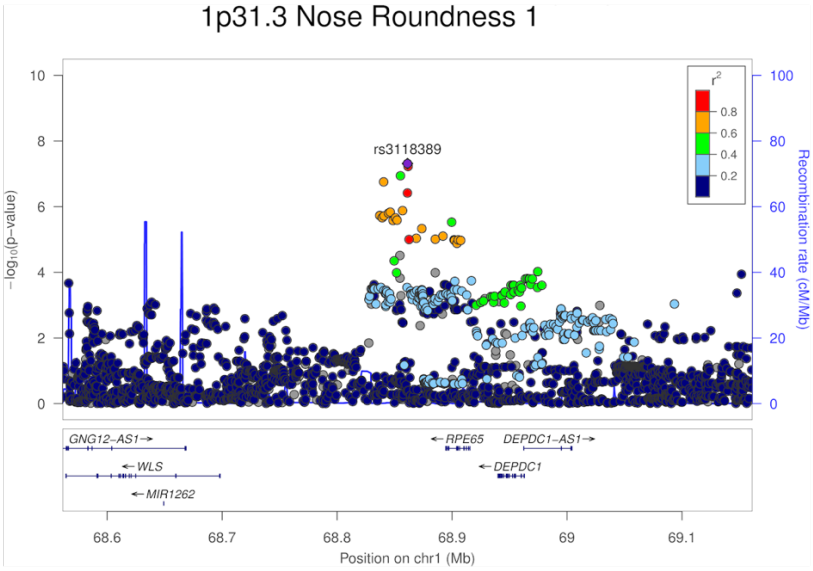

1p31.3: *RPE65, DEPDC1*. We associated a SNP from *RPE65* (retinoid isomerohydrolase *RPE65*) and *DEPDC1* (DEP domain containing 1) region with nose roundness. This region has already been associated with orbital, midface and chin area *(11)*.

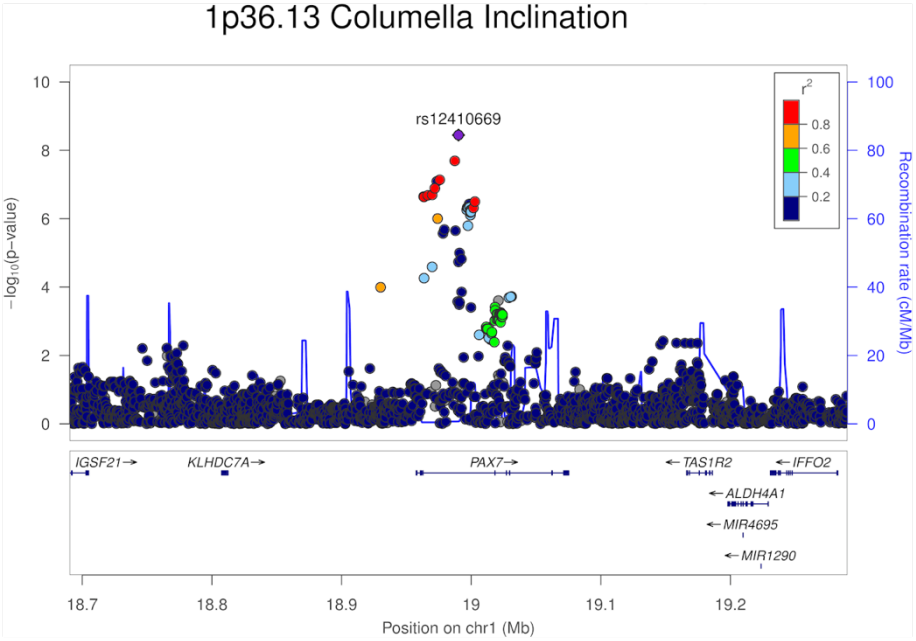

1p36.13: *PAX7*. We associated SNPs within PAX7 (paired box 7) gene with columella inclination. 1p36 region has been associated with the nose tip shape and the angle between the lips and the nose *(12)*. Homozygous mutations in the PAX7 gene can induce progressive congenital myopathy with scoliosis (MYOSCO) (OMIM #618578). People with this condition present particular facial phenotypes: posteriorly rotated and low set ears, flat nose and hypotonic triangular.

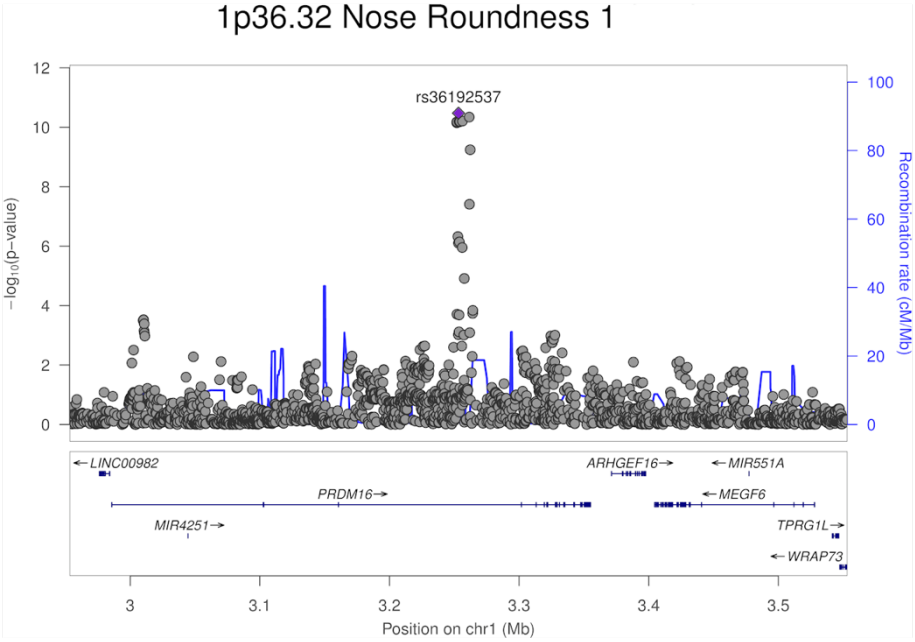

1p36.32: *PRDM16*. We associated SNPs within PRDM16 (PR/SET domain 16) gene with nose size and nose roundness. SNPs from this gene has already been associated with nose phenotypes (nose width and nose height) *(2)*.

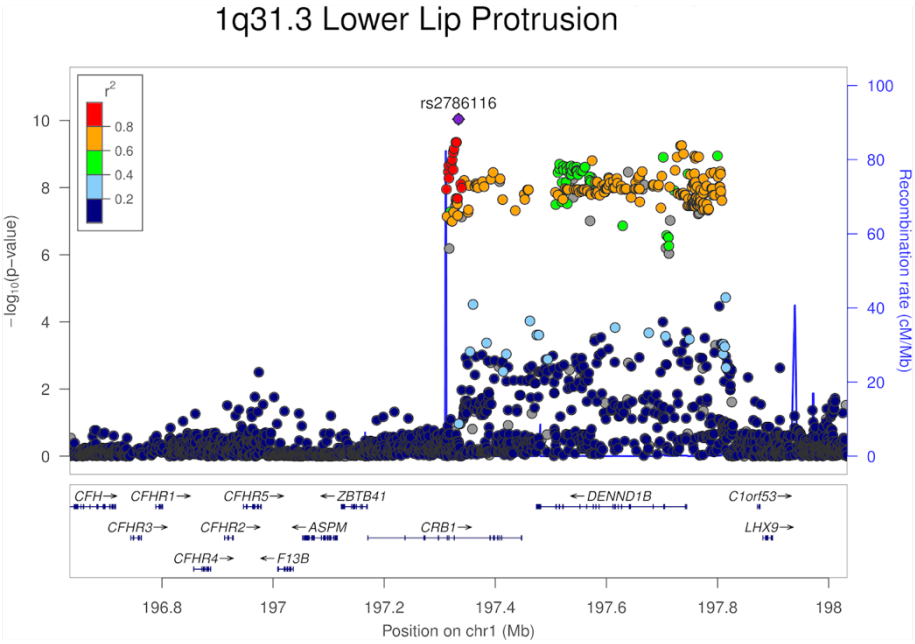

1q31.3: *CRB1, DENND1B*. We associated SNPs from *CRB1* (crumbs cell polarity complex component 1) and *DENND1B* (DENN domain containing 1B) region with lip, lower lip and chin protrusion. This region has already been associated with chin related phenotypes *(7,10)*.

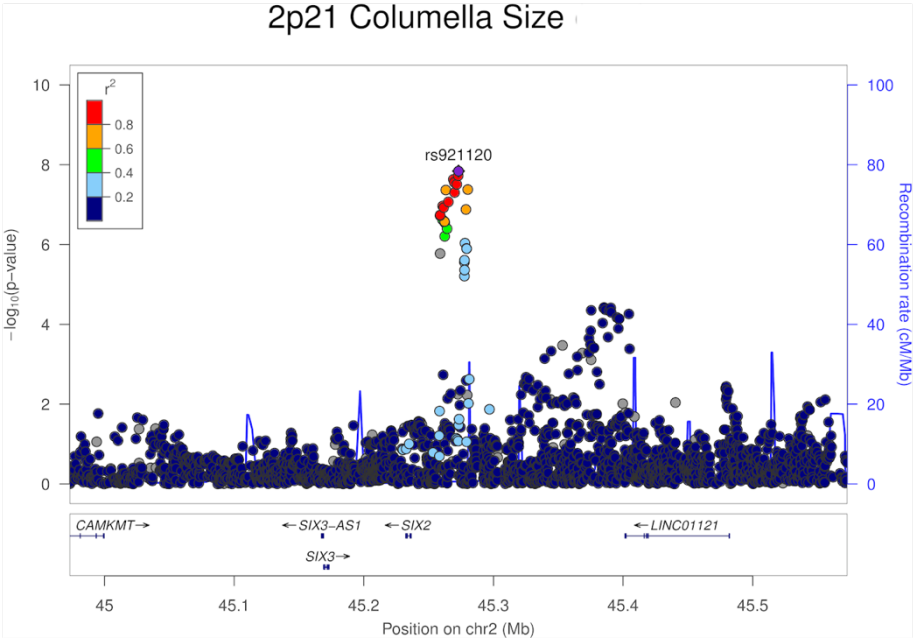

2p21: Intergenic (*SIX3, SIX2, LINC01121*). We associated SNPs from 2p21 region with columella size. This region has already been associated with facial variations *(2, 59)* and particularly with the chin morphology *(7,10,12)*. Before that, this region was known to have an impact on facial morphology because it was associated with non-syndromic cleft lip with or without cleft palate (NSCL/P) *(71)*. Mutations in this region can induce holoprosencephaly 2 (OMIM #157170).

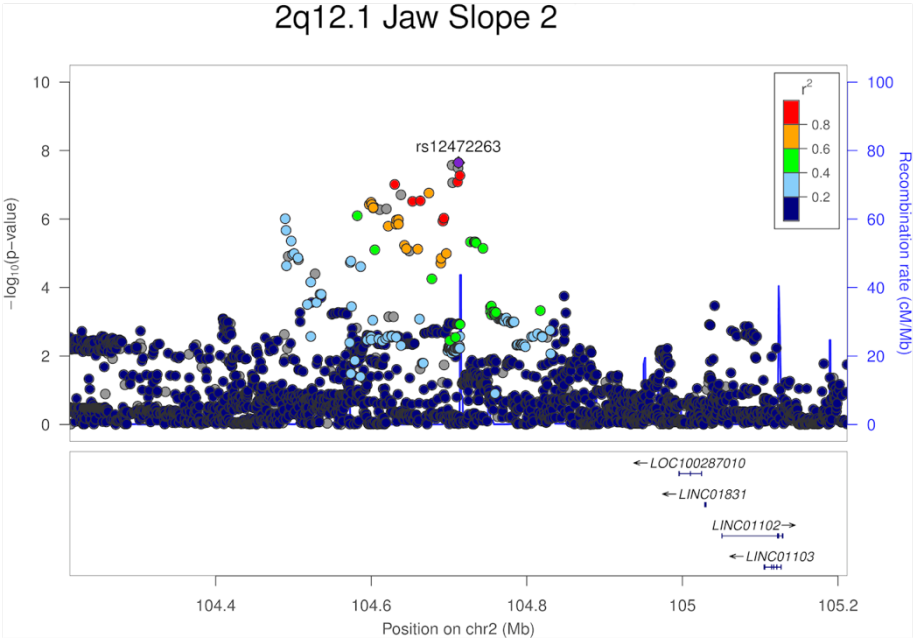

2q12.1: Intergenic (*LOC1002287010*). We associated SNPs from 2q12.1 region with jaw slope. This region has already been associated with chin dimples *(7)*.

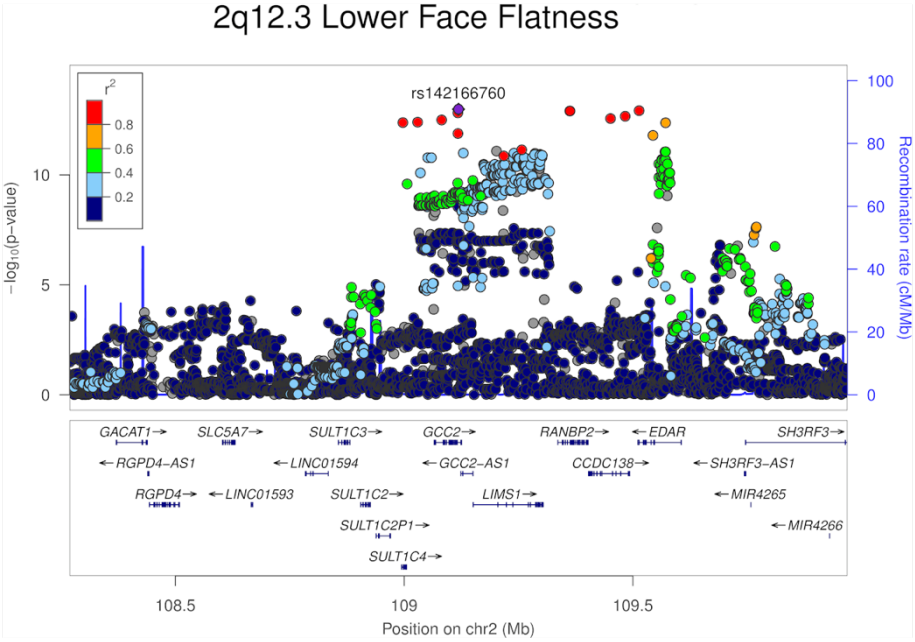

2q12.3: *EDAR* region. We associated SNPs from *EDAR* (ectodysplasin A receptor) region with lower lip protrusion, lower face flatness and jaw protrusion. This region has already been associated with chin and lips morphology in the CANDELA sample (and replicated in another study *(72)*) and with mandible and ear morphology in mutant mouse *(4)*. Mutations in the EDAR gene can induce ectodermal dysplasia (OMIM #224900). People with this condition can present particular skin and hair aspect as well as missing teeth.

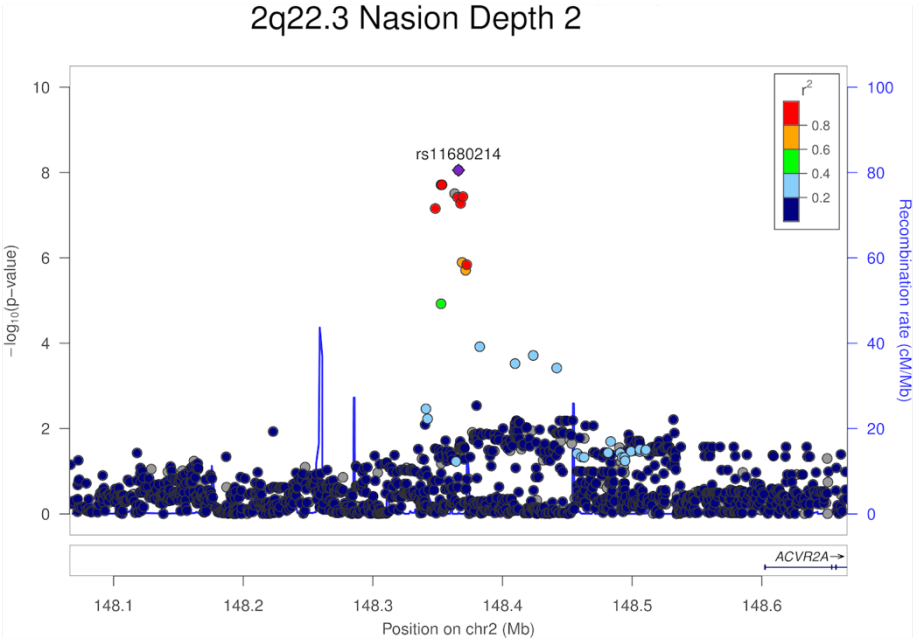

2q22.3: Intergenic (*ACVR2A*). We associated SNPs from the 2q22.3 region with nasion depth. SNPs from this region have been associated with chin dimples *(7)*.

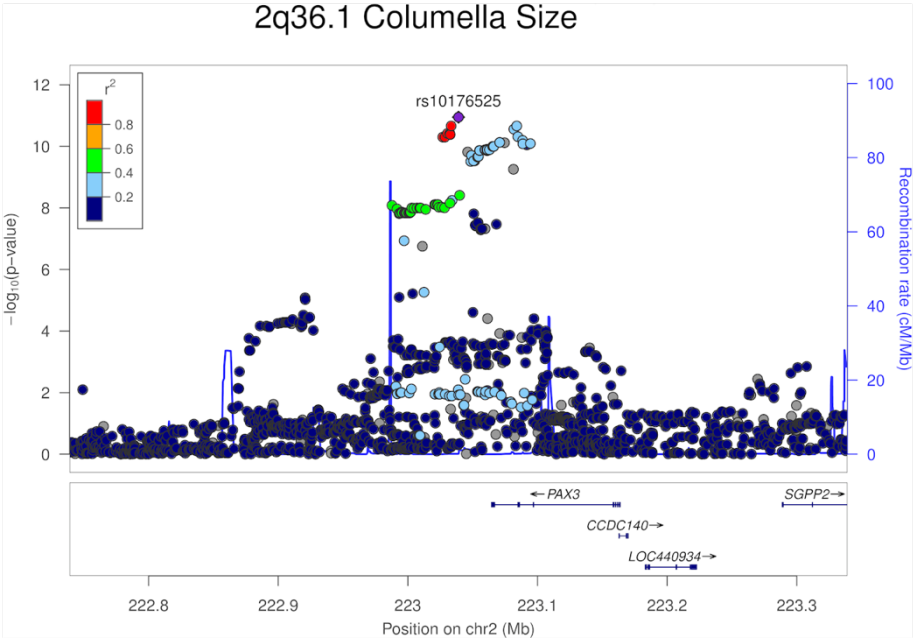

2q36.1: *PAX3*. We associated SNPs from *PAX3* (paired box 3) region with brow ridge protrusion, nasion depth, nasion position and columella size. *PAX3* has already been identified has having an effect on the nasion position *(1),* the nose area *(10)* and chin dimples *(7)*. Mutations in the PAX3 gene can induce craniofacial-deafness-hand-syndrome (CDHS) (OMIM #122880) and Waardenburg syndrome type 1 and 3 (OMIM #193500, #148820). People with those conditions can present particular facial phenotypes.

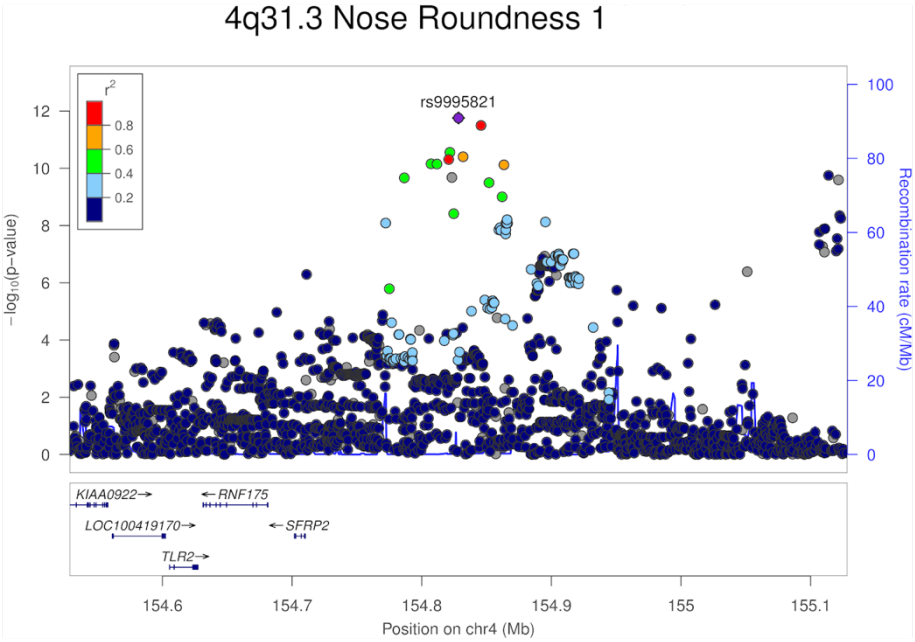

4q31.3: *SFRP2, DCHS2*. We associated SNPs from *SFRP2* (secreted frizzled related protein 2) and *DCHS2* (dachsous cadherin-related 2) region with nose height, nose roundness, columella inclination and nostril size. This region has already been associated with columella inclination and nose shape in general *(4,10)*.

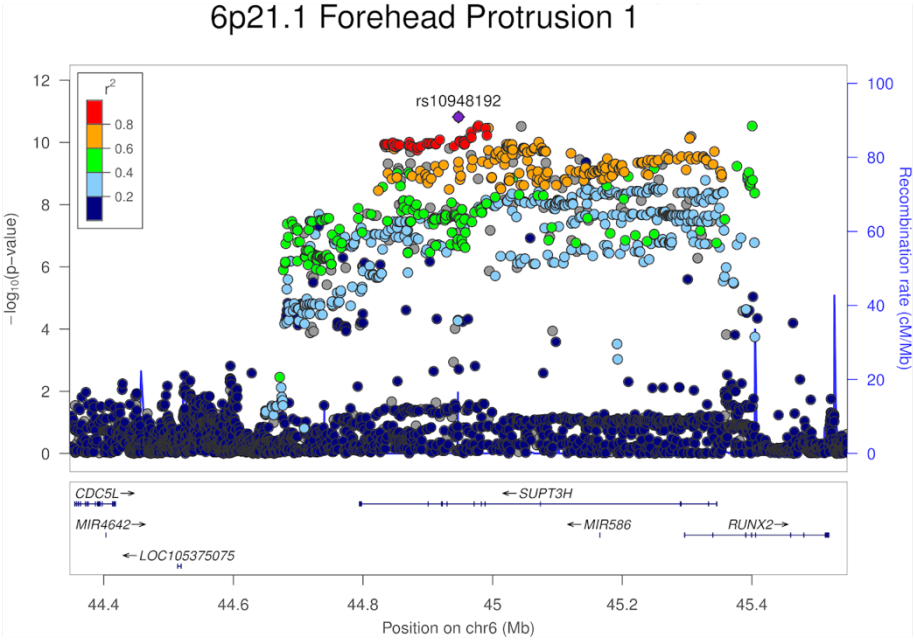

6p21.1: *SUPT3H, RUNX2*. We associated SNPs within SUPT3H (*SPT3* homolog, SAGA and STAGA complex component) and RUNX2 (RUNX family transcription factor 2) genes with forehead and brow ridge protrusion and upper face flatness. This region has already been associated with the nose bridge breadth in the CANDELA sample *(73)* and to nose morphology and chin dimples in other samples *(7,10)*. Mutations in RUNX2 gene can cause cleidocranial dysplasia (CDD) (OMIM #119600). People with this condition can present poor closure of the cranial sutures.

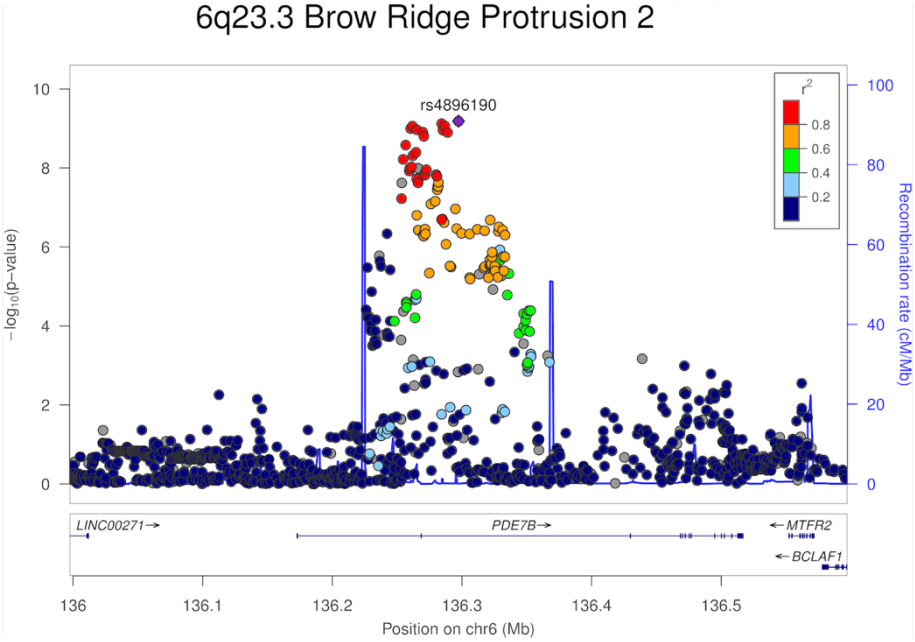

6q23.3: *PDE7B*. We associated SNPs within PDE7B (phosphodiesterase 7B) gene with brow ridge protrusion. The 6q23 region has already been associated with the upper part of the face *(10)*.

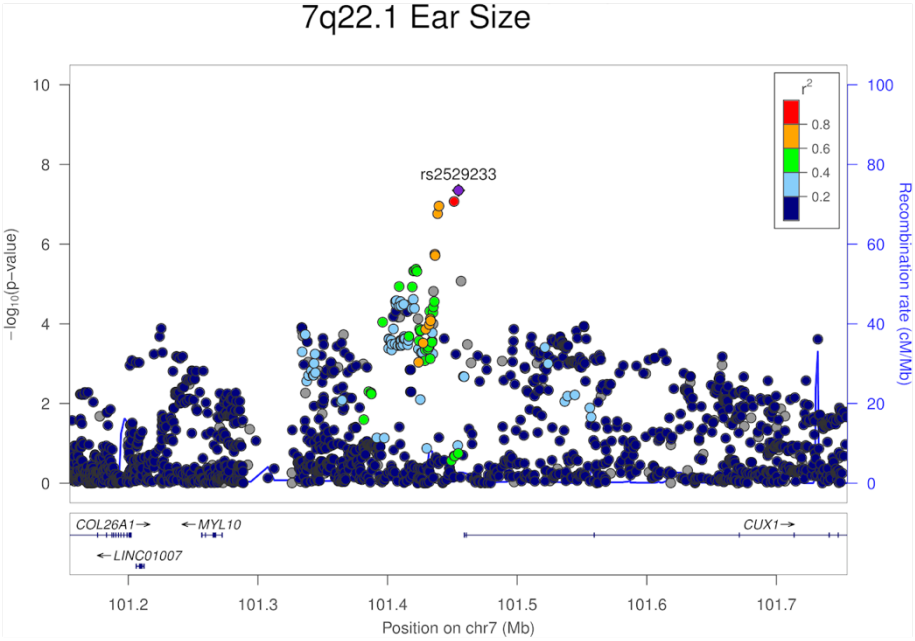

7q22.1: *CUX1*. We associated a SNP from *CUX1* (cut like homeobox 1) region with ear size. This region has already been associated with mid face area (eyes, nose, philtrum and lips) *(11)*. Mutation in the RELN gene, located in this region, can induce lissencephaly syndrome (OMIM #257320). People with this condition present a low sloping forehead and a salient nasal bridge.

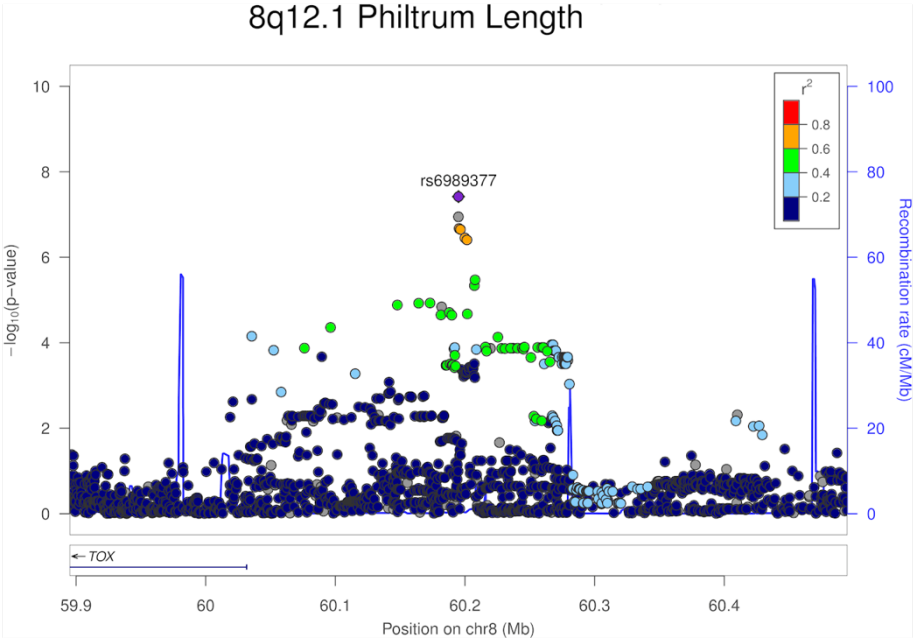

8q12.1: Intergenic (*TOX*). We associated a SNP from 8q12.1 region with philtrum length. This region has already been associated with the depth of nasal alae *(5).*

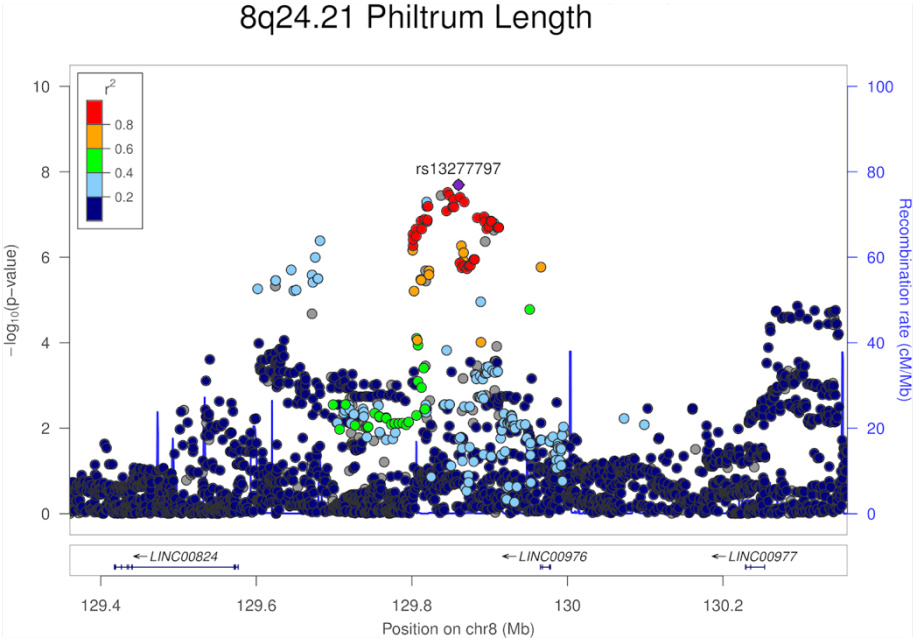

8q24.21: Intergenic (*LINC00976*). We associated SNPs from 8q24.21 region with philtrum length. This region has already been associated with facial distances *(2)* and with cleft lip with or without cleft palate *(62)*.

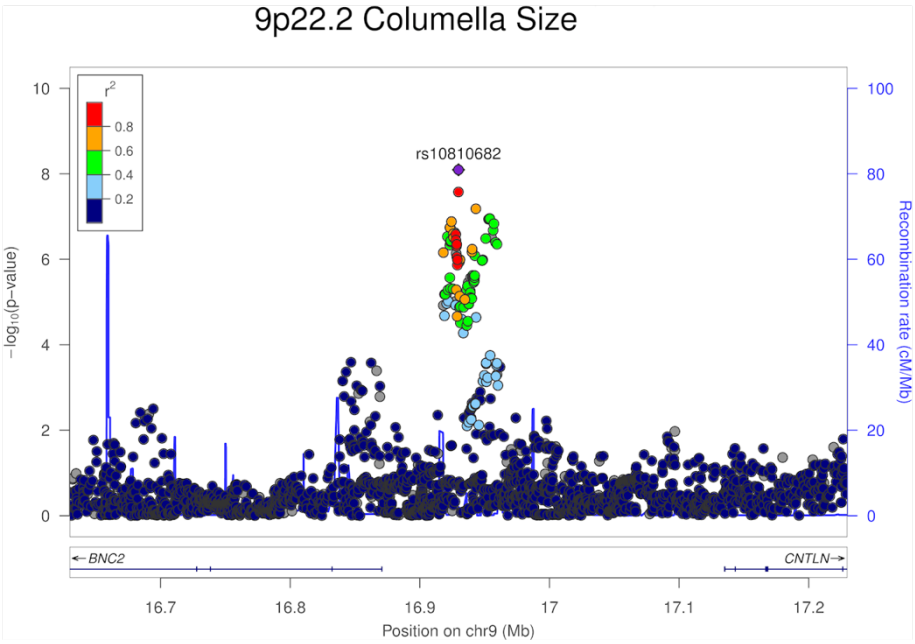

9p22.2: Intergenic (*BNC2, CNTLN*). We associated SNPs from 9p22.2 region with columella size. This region has already been associated with the height of the vermilion upper lip *(5)*.

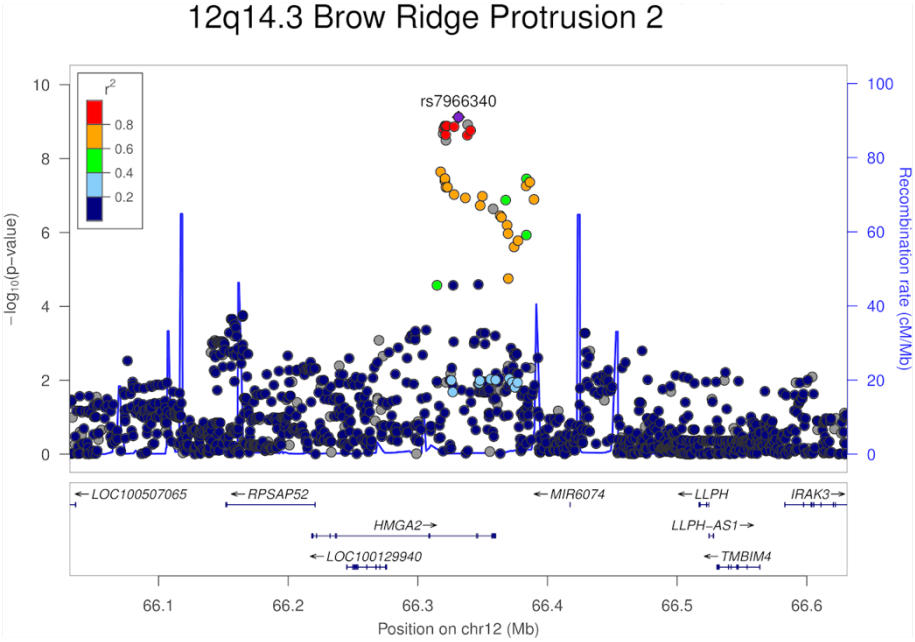

12q14.3: *HMGA2, MIR6074*. We associated SNP from *HMGA2* (high mobility group AT-hook 2) and *MIR6074* (microRNA 6074) region with forehead and brow ridge protrusion. This region has already been associated with chin dimples *(7)* and craniofacial distances *(74)*.

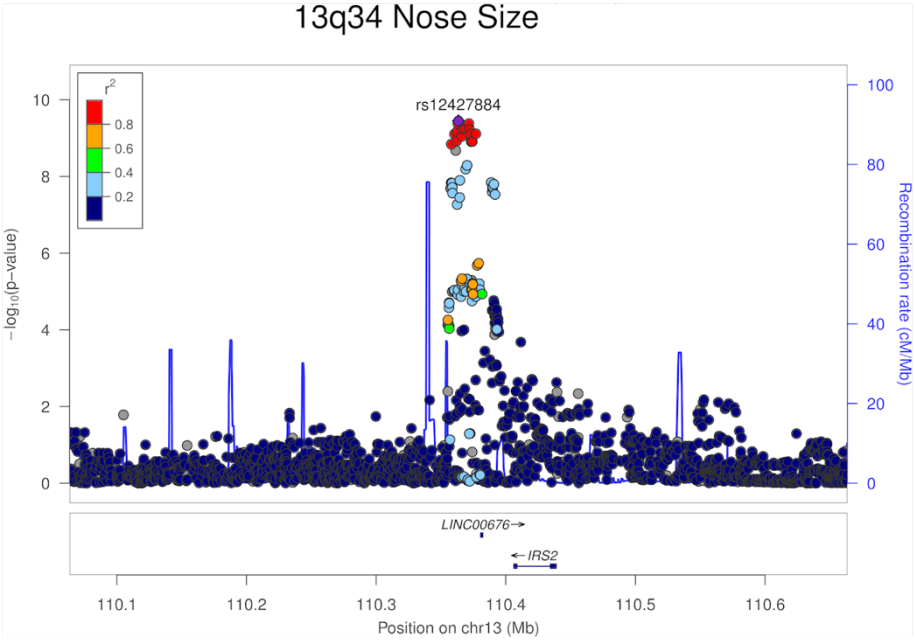

13q34: *LINC00676, IRS2*. We associated SNPs from *LINC00676* (long intergenic non-protein coding RNA 676) and *IRS2* (insulin receptor substrate 2) region with protrusion and size of the nose. The 13q34 region has already been associated with the nose size *(7)*.

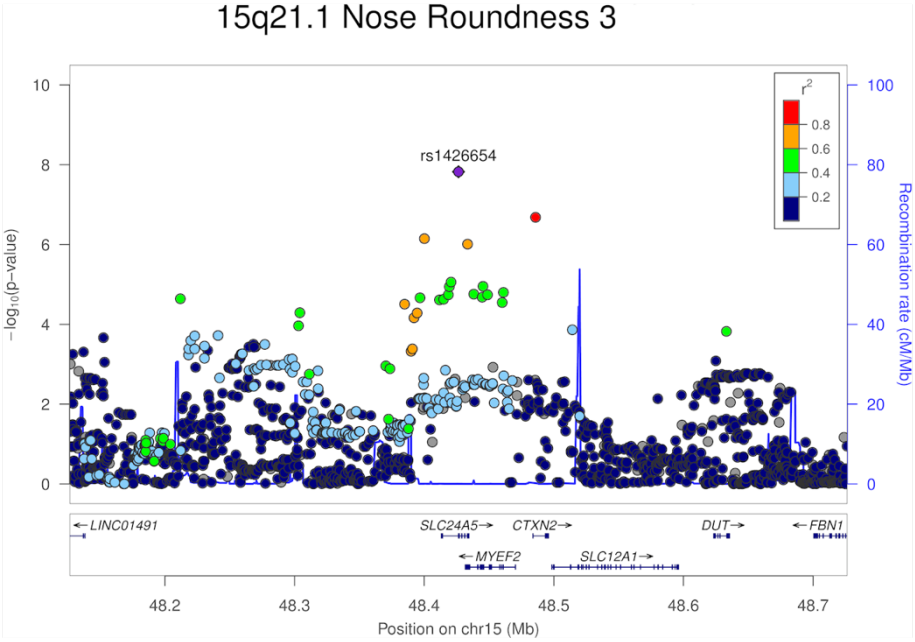

15q21.1: *SLC24A5, MYEF2*. We associated SNPs from *SLC24A5* (solute carrier family 24 member 5) and *MYEF2* (myelin expression factor 2) region with nose roundness and columella inclination. The 15q21.1 region has already been associated with facial morphology (mouth corners, lateral parts of the mandible, philtrum, medial parts of the midface, eyes and forehead) *(11)*. Mutations in the 15q21 region can induce Marfan syndrome (OMIM #154700). People with this condition presents particular facial and skeletal features.

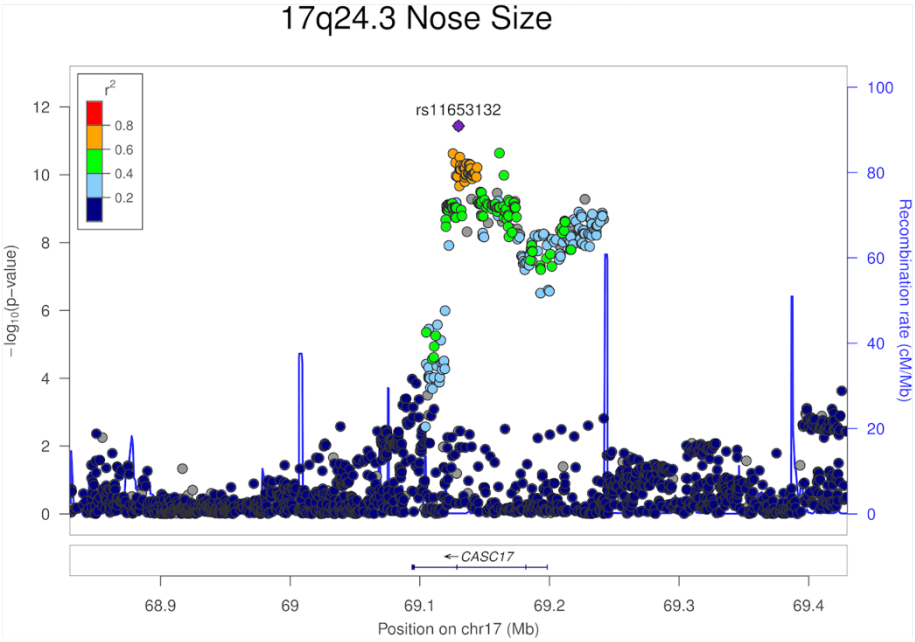

17q24.3: *CASC17*. We associated SNPs within CASC17 (cancer susceptibility 17) gene with roundness and size of the nose, as well as columella inclination. This region has already been associated with nose morphology *(7,10)*.

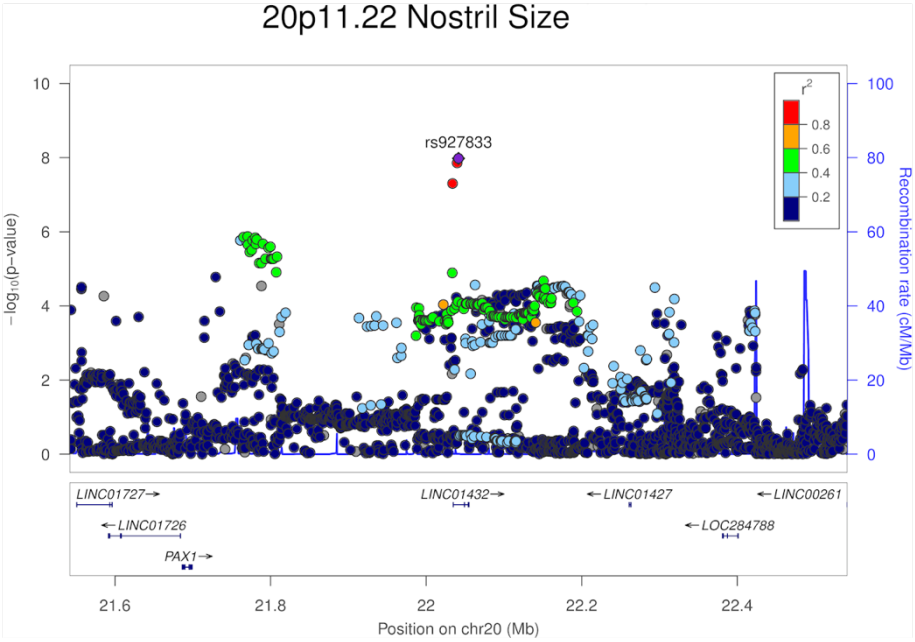

20p11.22: *LINC01432*. We associated SNPs from the 20p11.22 region with nostril size. This region has already been associated with the nasal area *(4,6,10).*

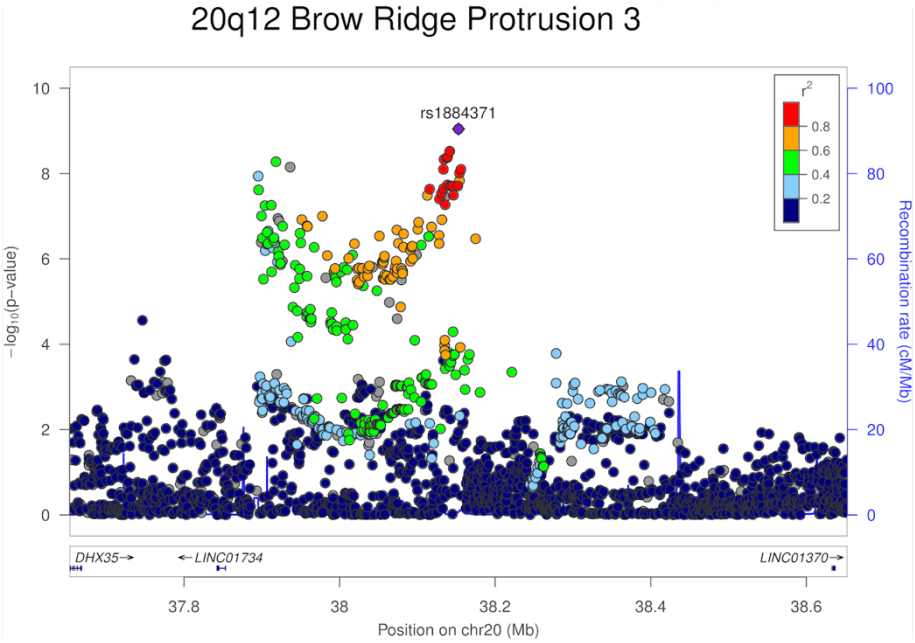

20q12: Intergenic (*LINC01734, DHX35)*. We associated SNP from the 20p12 region with brow ridge protrusion. This region has already been associated with chin dimples, nose size *(7)*, cranial base width *(6)* and cleft lip with and without cleft palate *(73).*

Supplementary note: Regional association plots for the 5 novel regions detected here that do not replicate in the European GWAS meta-analysis

Gene locations, Pairwise LD, and annotations for regulatory elements active during craniofacial development are also shown.

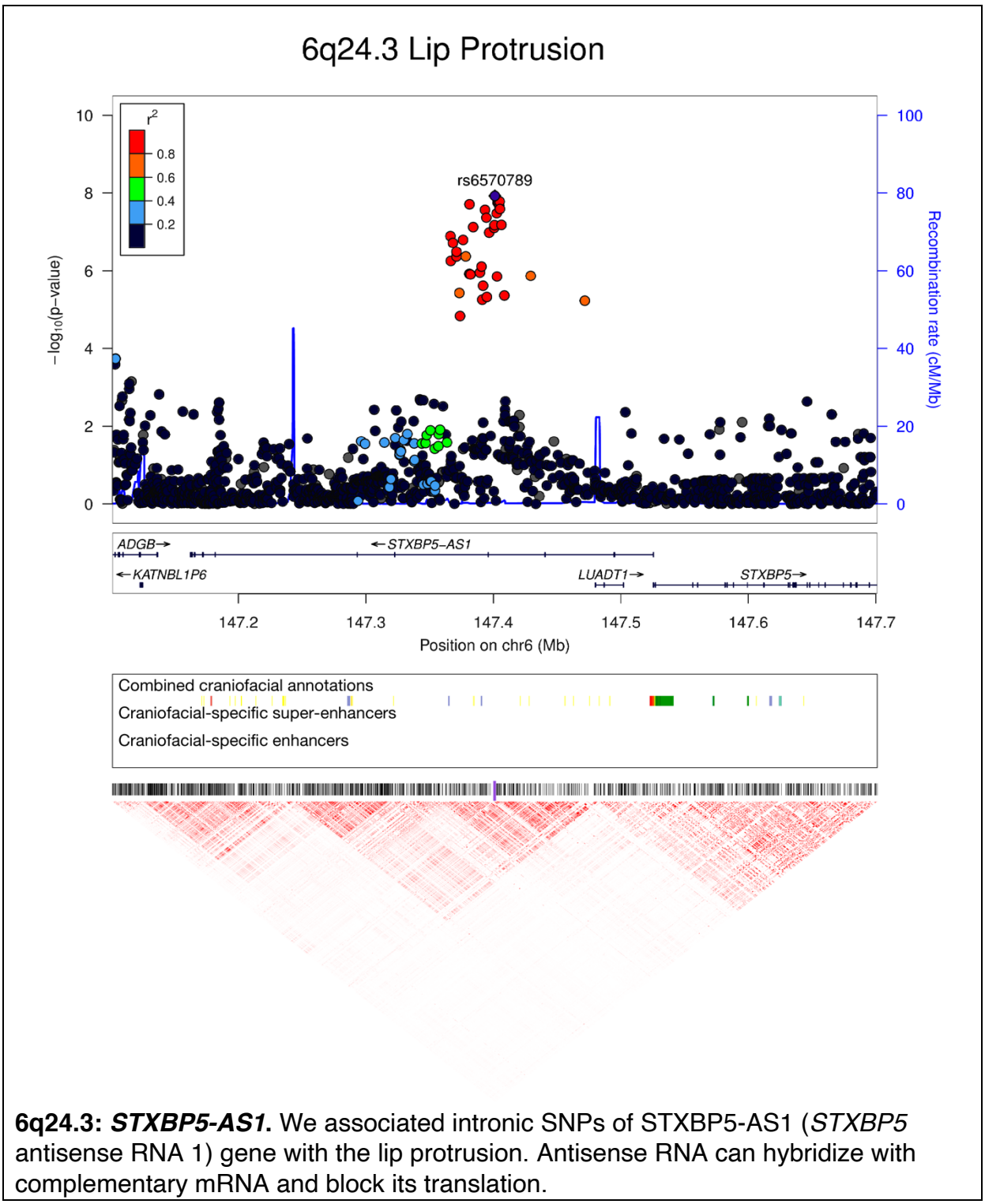

6q24.3: *STXBP5-AS1*. We associated intronic SNPs of STXBP5-AS1 (*STXBP5* antisense RNA 1) gene with the lip protrusion. Antisense RNA can hybridize with complementary mRNA and block its translation.

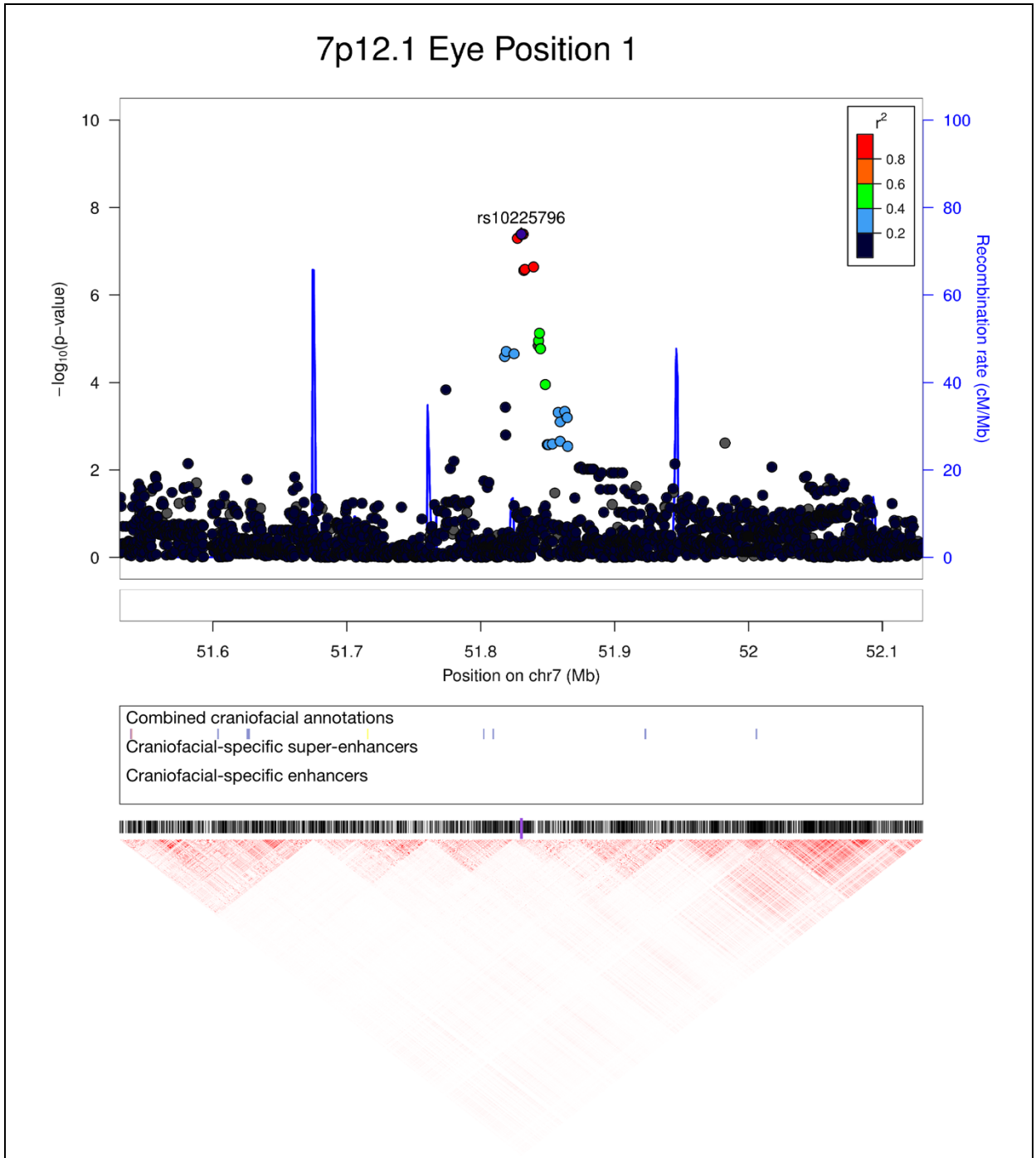

7p12.1: Intergenic (*COBL*). We significantly associated three intergenic SNPs in 7p12.1 with eye position. Closest entity is a pseudogene RN7SL292P (RNA, 7SL, cytoplasmic 292, pseudogene) situated about 50,000BP upstream. In the region, there is also COBL (cordon-bleu WH2 repeat protein) gene about 445,000BP upstream. This gene encodes for an actin nucleator protein. In zebra fish, Cobl is mainly expressed in brain and retina, it seems to be essential in the formation of cilia (hair-like structure of the surface of cells). Defect in the cilia formation can induce developmental error, like failures in left/right patterning *(75)*. It appears that primary cilium has central part in vertebrate development and various human genetic diseases *(76)*.

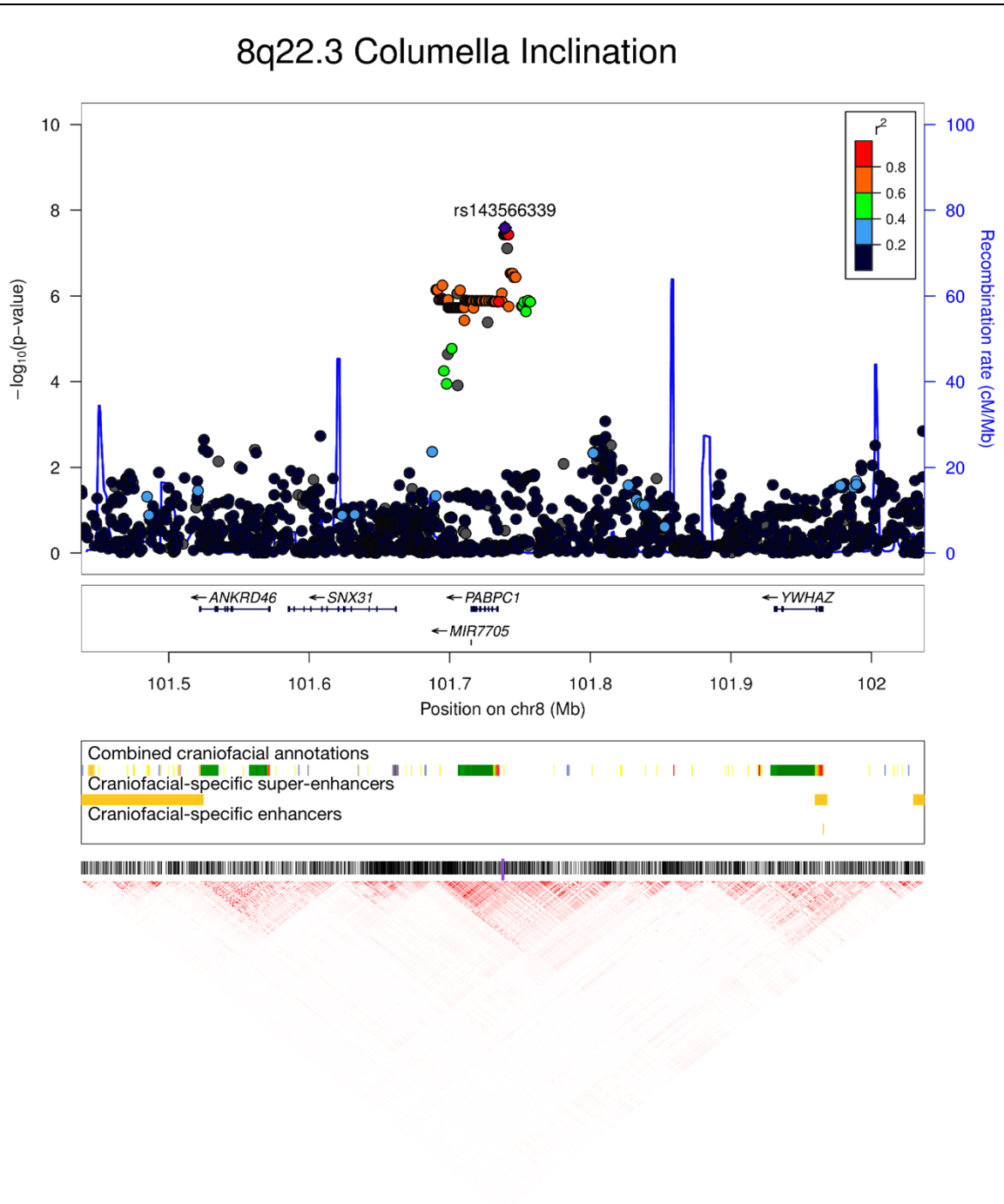

8q22.3: *PABPC1.* We significantly associated intronic variants of *LOC105375673* with columella inclination and suggestively with nose roundness. The most significant variant was an indel 8:101737776:AT:ATT. Around 1,000BP upstream there is PABPC1 gene (poly(A) binding protein cytoplasmic 1), it encodes for a poly(A)-binding protein that plays a role in translation.

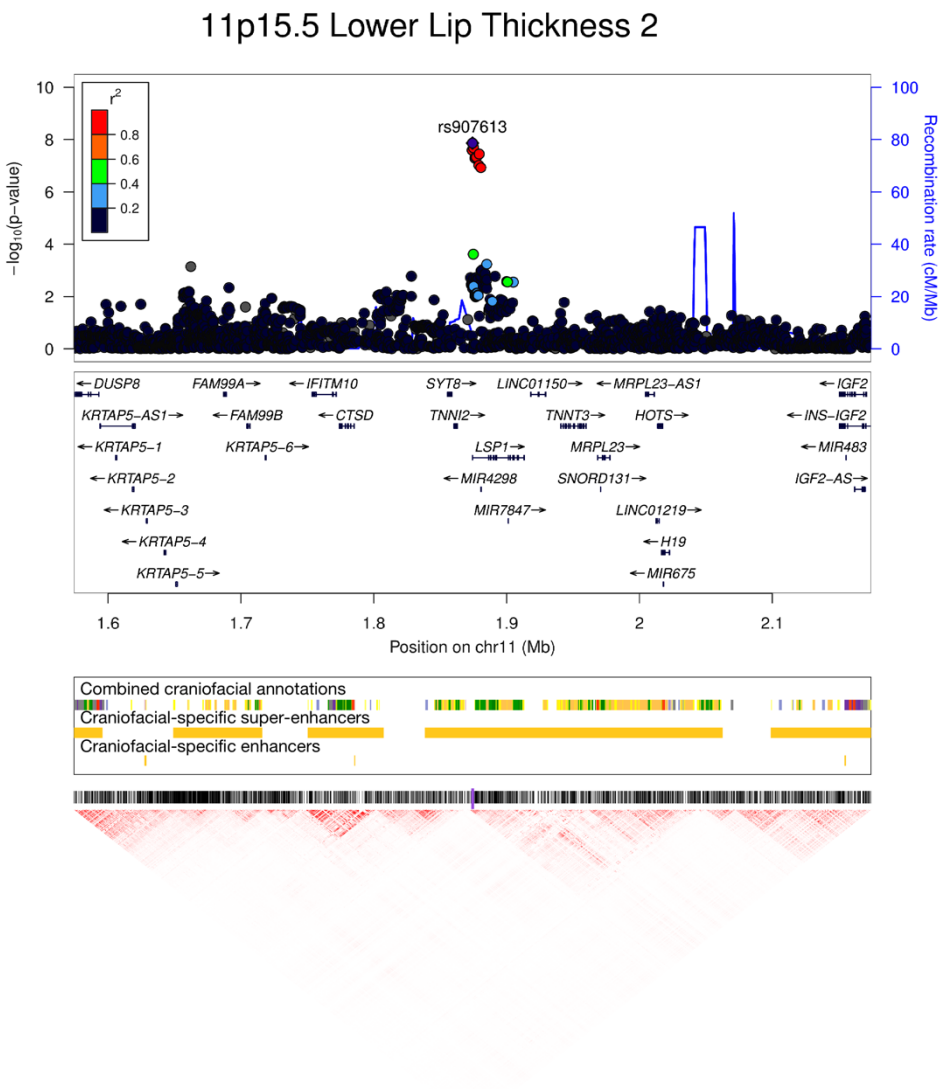

11p15.5: ***LSP1.*** We significantly associated intronic SNPs from LSP1 gene with lip thickness and lower lip thickness. But most significant one was rs907613 a variant situated 2KB upstream *LSP1*. LSP1 stands for lymphocyte specific protein 1. This gene has been associated with multiple traits including systolic blood pressure *(35)*, and height *(35)*. There are also craniofacial specific super-enhancers and multiple gene in that region. Among them there is *TNNI2* (Troponin I2, Fast Skeletal Type) which encodes for troponin I protein found in skeletal muscle. In mice this gene seems to have an effect in the regulation of bones development *(77).* There is also *TNNT3* (troponin T3, fast skeletal type), a gene that encodes for an isoform of troponin T that play a crucial role in the contraction and relaxation of fast skeletal muscle *(78).* Additionally, in that region there is a cluster of imprinted genes, among them there is *IFG2* (Insulin Like Growth Factor 2) a gene that regulates skeletal growth *(79)* and *H19* (H19 imprinted maternally expressed transcript). Different epigenetic mechanisms can affect the expression of those two genes resulting in two opposite growth disorder: Beckwith-Wiedemann syndrome (OMIM #130650), which is defined by pre and postnatal overgrowth and macroglossia (large tongue) and Silver-Russell syndrome (OMIM #616489), which is defined among other by growth retardation and craniofacial features like broad forehead and triangular shaped face.

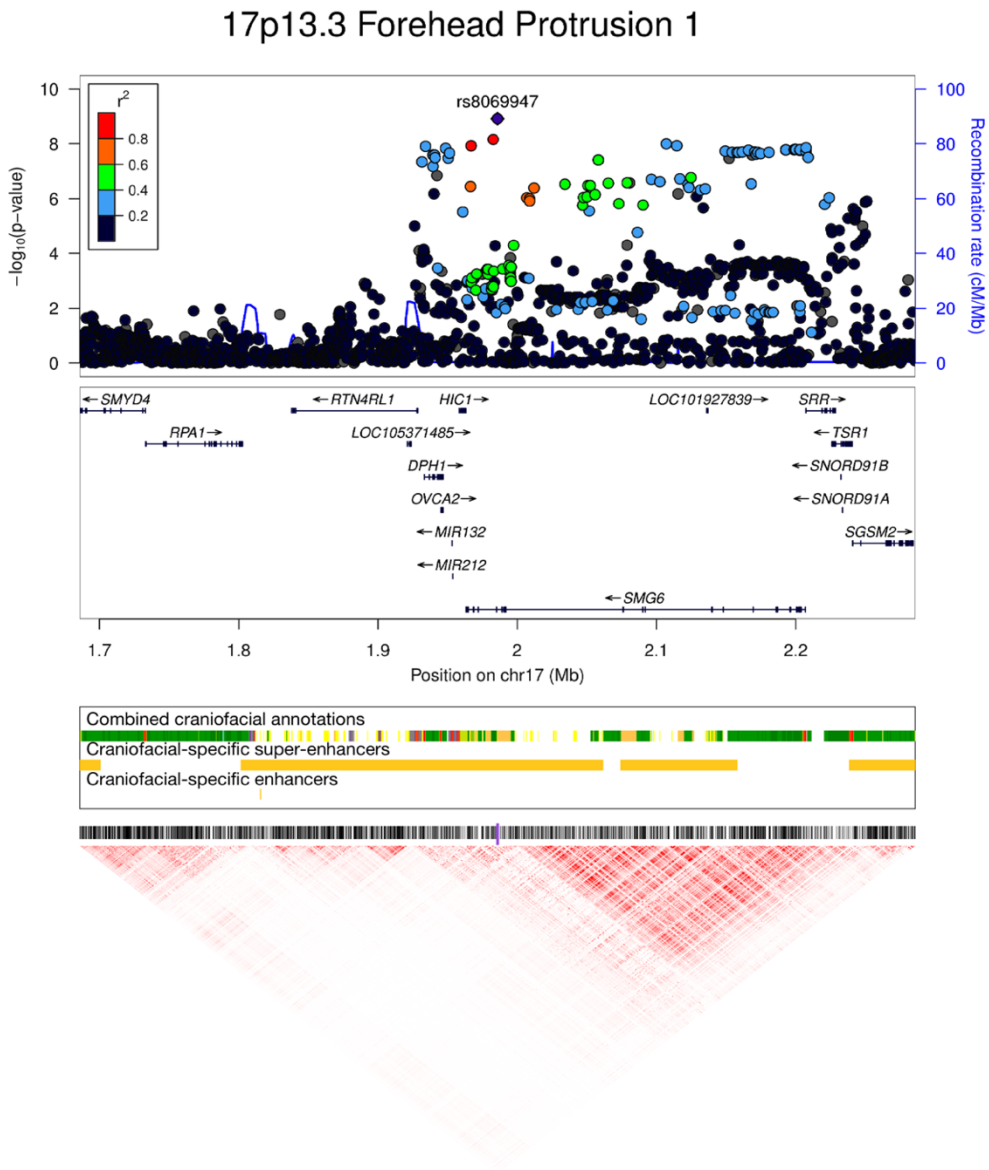

17p13.3: *SMG6.* We significantly associated 41 variants from 17p13.3 region with forehead protrusion. One was 2KB upstream *DPH1* (diphthamide biosynthesis 1), four were intron variants of *DPH1*, 3 were intron variants of *SRR (serine racemase),* 26 were intron variants of *SMG6 (SMG6* nonsense mediated mRNA decay factor) and 2 were missense variant of *SMG6*: rs1885987 (an asparagine becomes a serine or a threonine) and rs1885986 (an arginine becomes a proline) both in exon 2 or 3 out of 30. The most significant SNP was rs8069947 an intronic variant of SMG6 gene. *SMG6* encodes for a protein link with telomerase activity. In zebrafish, SMG6 protein contributes to a mechanism that detects and degrades mRNAs with premature stop codons and is needed for proper embryonic development *(80).* SNPs from this gene have been associated with multiple traits including height *(35)*. It also has been suggestively associated with forehead morphology *(9)* and we found suggestive association with eyebrow protrusion. This region includes several craniofacial super-enhancers.

Supplementary note: Geometric morphometrics analysis of mouse skulls

Landmarks and semi-landmarks used

A set of 44 landmarks and curve semi-landmarks were digitized on meshes using the R package digit3DLand vs 0.1.5 (https://github.com/morphOptics/digit3DLand). This set is composed of 11 paired landmarks and 4 unpaired landmarks. Many skulls have their posterior part damaged due to brain removal and landmarks were limited to the face and the palate. Seven additional curve paired semi-landmarks and five unpaired curve semi-landmarks modeling the nasal bone curvature as well as the nasal vestibule opening were also digitized (Figure S3-1).

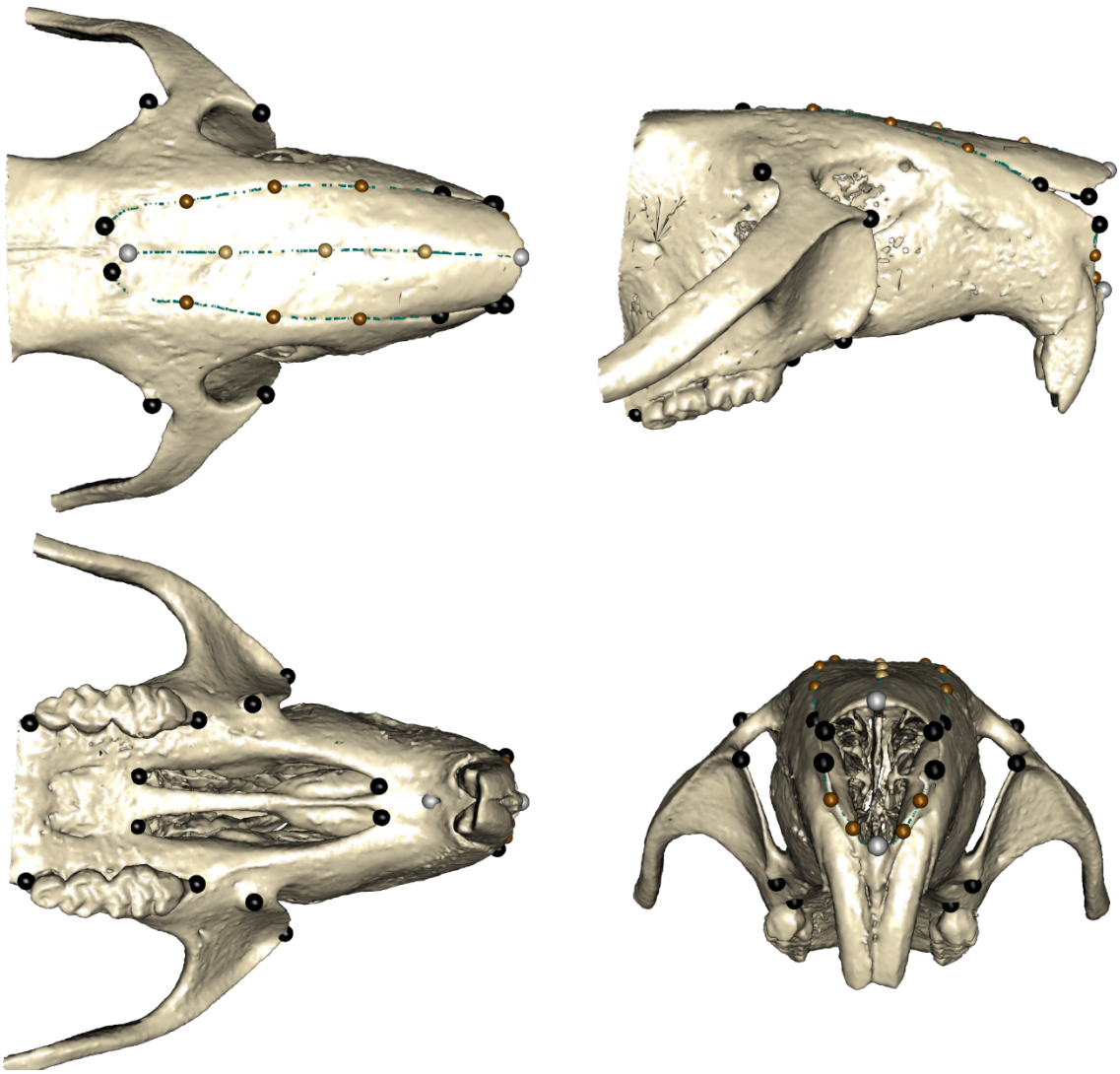

Figure S3-1. The landmarks and curve semi-landmarks used for the analysis. Black dots are the 11 paired landmarks and gray dots are four unpaired landmarks. Dark orange dots are seven paired curve semi-landmarks and light orange are five unpaired curve semi-landmarks. Curves are green lines.

Vps13b KO mice are smaller and lighter than WT especially in males

The KO and gender effects on body length were analyzed in a linear model based on a subsample of 36 mice. The interaction between genotype and gender is significant ($F_{1, 32} = 8.65$, $p = 0.006$), and the KO effect appearing stronger in male than female (Supplementary Fig. S3-2). Altogether genotype effects explain 39% of the variance in body length. In the linear modelling of the log-transformed body weight, and after controlling for body length ($F_{1, 31} = 16.05$, $p = 0.00036$), and gender ($F_{1, 31} = 57.93$, $p = 1.39 \times 10^{-8}$), the genotype has an effect ($F_{1, 31} = 34.44$, $p = 1.78 \times 10^{-6}$) with KO mice being lighter than WT mice. Interaction between gender and genotype was kept in the model but it was almost identical than dropping it (ΔAIC = 0.73). The full model shows a slightly stronger effect in male than in female (Supplementary Fig. S3-2) but this could result from chance alone ($F_{1, 31} = 2.45$, $p = 0.13$) and it will need additional data. Altogether genotype effects explain 26% of the variance in body weight once controlled for body size.

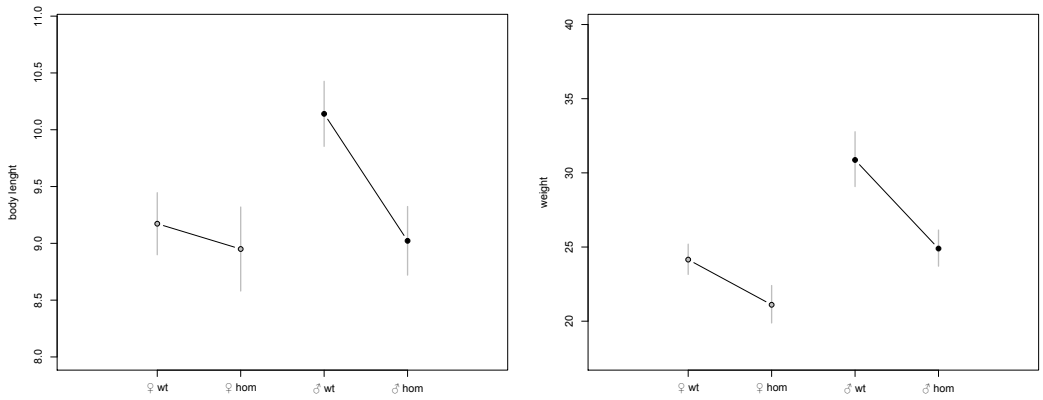

Figure S3-2. Expected marginal means of the body length or weight in 19 weeks old Vps13b mice. The weight model includes body length as an additional covariates and marginal means are predicted at the population average body length. Error bars correspond to 95% confidence interval.

Vps13b KO mice have smaller facial and palatal size than WT

The KO and gender effects on body length were analyzed in a linear model. Body length was initially included as covariate together with gender and genotype, but it was dropped from the model (ΔAIC = -1.67), as well as the interaction between gender and genotype (ΔAIC = -0.17). Genotype has a strong main effect explaining 53.7% of the variance in facial centroid size (Table S3-1 and Figure S3-3)

Table S3-1. ANOVA of centroid size

Sources	Df	SS	MS	r^2	F	Pr(>F)
sex	1	1.24	1.24	0.09	3.40	0.0079
genotype	1	7.60	7.60	0.54	45.41	4.73×10^{-8}
Residuals	34	5.30	0.16			

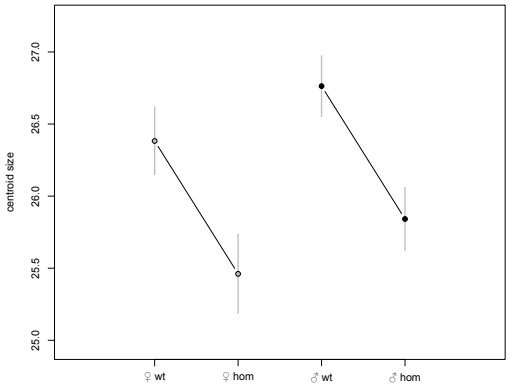

Figure S3-3. Expected marginal means of the facial centroid size in Vps13b mice. Error bars correspond to 95% confidence interval.

Table S3-2. Procrustes ANOVA of shape variation in *Vps13b* KO-mutant and Wild-type mice

	Df	SS (× 10^{-3})	MS (× 10^{-3})	r^2	*F*	Pr(>SS)
Size	1	1.69	1.69	0.063	2.89	0.026
Sex	1	2.37	2.37	0.089	4.06	0.005
Genotype	1	1.54	1.54	0.058	2.64	0.021
Sex × genotype	1	1.37	1.37	0.052	2.35	0.016
Residual	32	18.68	0.58			

Supplementary Movie 1. Movies of the Vps13b KO effect in males. A threefold scaling of the effect is visualized at the maximum. Effect is predicted according to the expected marginal means at the population average centroid size.

Supplementary Movie 2. Movies of the effect at the Vps13b locus in outbred mice. The effect is scaled by 50 when visualized at the maximum.

Supplementary figures

Supplementary figure S1: Landmarking protocol

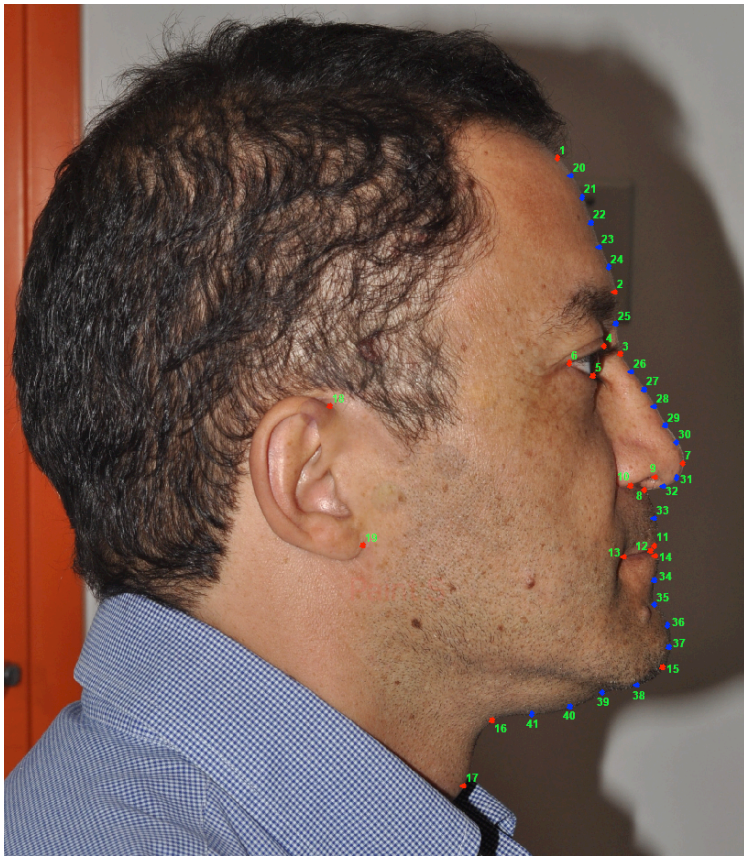

Photo Credit: William Arias, GENMOL (Genética Molecular), Universidad de Antioquia, Medellín, Colombia.

Landmarks (L) are shown in red and Semi-Landmarks (SL) in blue

1 Trichion or Crinion (T)
2 Glabella (G)
3 Nasion (N)
4 Palpebral superiorus (Ps)
5 Palpebral inferiorus (Pi)
6 Exocanthion (ExR)
7 Pronasale (Prn)
8 Subnasale (Sn)
9 Nostril superiorus (Nos)
10 Nostril inferiorus (Noi)
11 Labial superiorus (Ls)
12 Stomion (St)
13 Cheilion (ChR)
14 Labial inferiorus (Li)
15 Pogonion (Po)
16 Neck start (NS)
17 Adam's apple (A)
18 Otobasion superiorus (Os)
19 Otobasion inferiorus (Oi)

Supplementary figure S2: GREGOR enrichment analysis for enhancer annotations and CANDELA face profile GWAS hits.

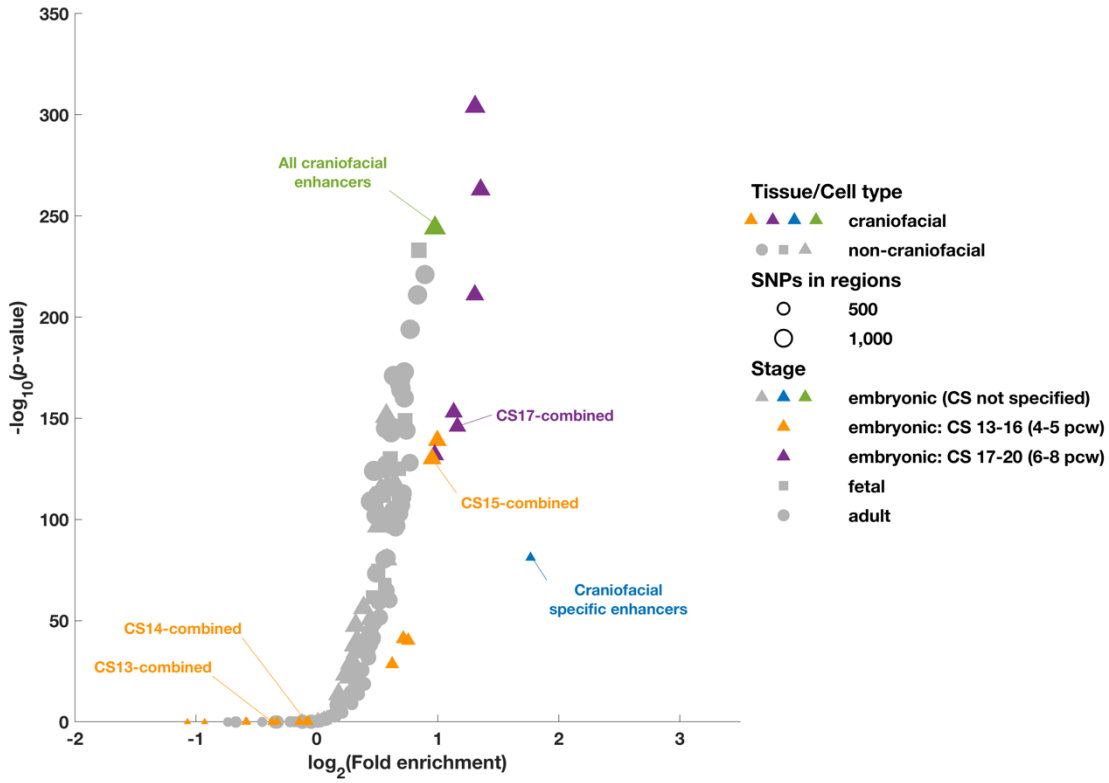

We tested for enrichment of profile GWAS hit SNPs relative to randomly selected control SNPs using an LD aware approach (see https://genome.sph.umich.edu/wiki/GREGOR) in enhancers annotated by ChromHMM using a 25 state chromatin model. We utilized harmonized annotations reported for 127 non-craniofacial tissue samples/cell types studied by the Roadmap Epigenomics Consortium *(67)* (grey symbols) and for craniofacial tissue from 17 human embryos *(27)* (orange symbols). Individual craniofacial tissue samples are labelled according to Carnegie Stages (CS13-20 referring to 4-8 post-conception weeks (pcw)), with annotations for a particular stage combined across individual replicates. Enrichment of GWAS hits was also tested for all enhancers detected in craniofacial tissue (across CS stages, in green), and for the subset of these enhancers that are detected in craniofacial tissue but not in Roadmap Epigenomics data (Craniofacial-specific enhancers, in blue). Symbol size is proportional to number of profiles GWAS hit SNPs identified in enhancer annotations for each tissue sample/cell type, as determined by GREGOR (*28*). The *y*-axis is the -$\log_{10}$ transformation of Bonferroni corrected *p*-values reported by GREGOR based on number of samples tested (n=150). The *x*-axis is the $\log_2$ transformation of fold enrichment of observed GWAS hit SNPs in a given tissue enhancer set relative to an equally sized but randomly selected number of SNPs. An *x*-axis value of 1 means that there are twice as many associated SNPs in the genome region with the specified annotation than expected assuming a uniformly random distribution of associated SNPs in the genome.

Supplementary figure S3: Cumulative counts of Denisovan haplotypes estimated at various confidence levels

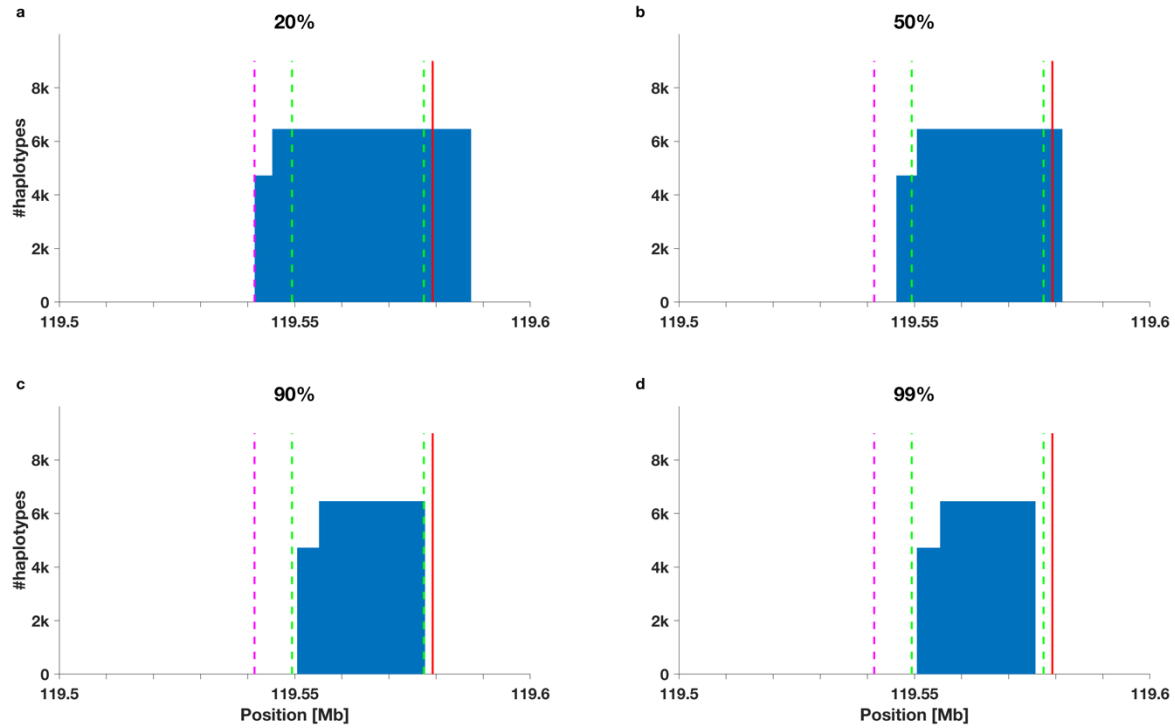

The region shown spans from 119.5 to 119.6Mb on chromosome 1. Haplotypes are counted over the whole CANDELA population (14,052 chromosomes); only haplotypes with MAF>1% are shown. With Denisovan sample as archaic reference, two haplotypes of decreasing lengths are called at increasing confidence thresholds (a: >20%, b: >50%, c: >90% and d: >99%). Annotations: position of the leading SNP (rs3790553) for lip thickness ratios (red vertical line), CRF (magenta dashed line) and HMM (green dashed line) tract bounds reported in Greenlandic Inuits *(31)*.

Supplementary figure S4: Association of the Denisovan tract to the 59 profile traits.

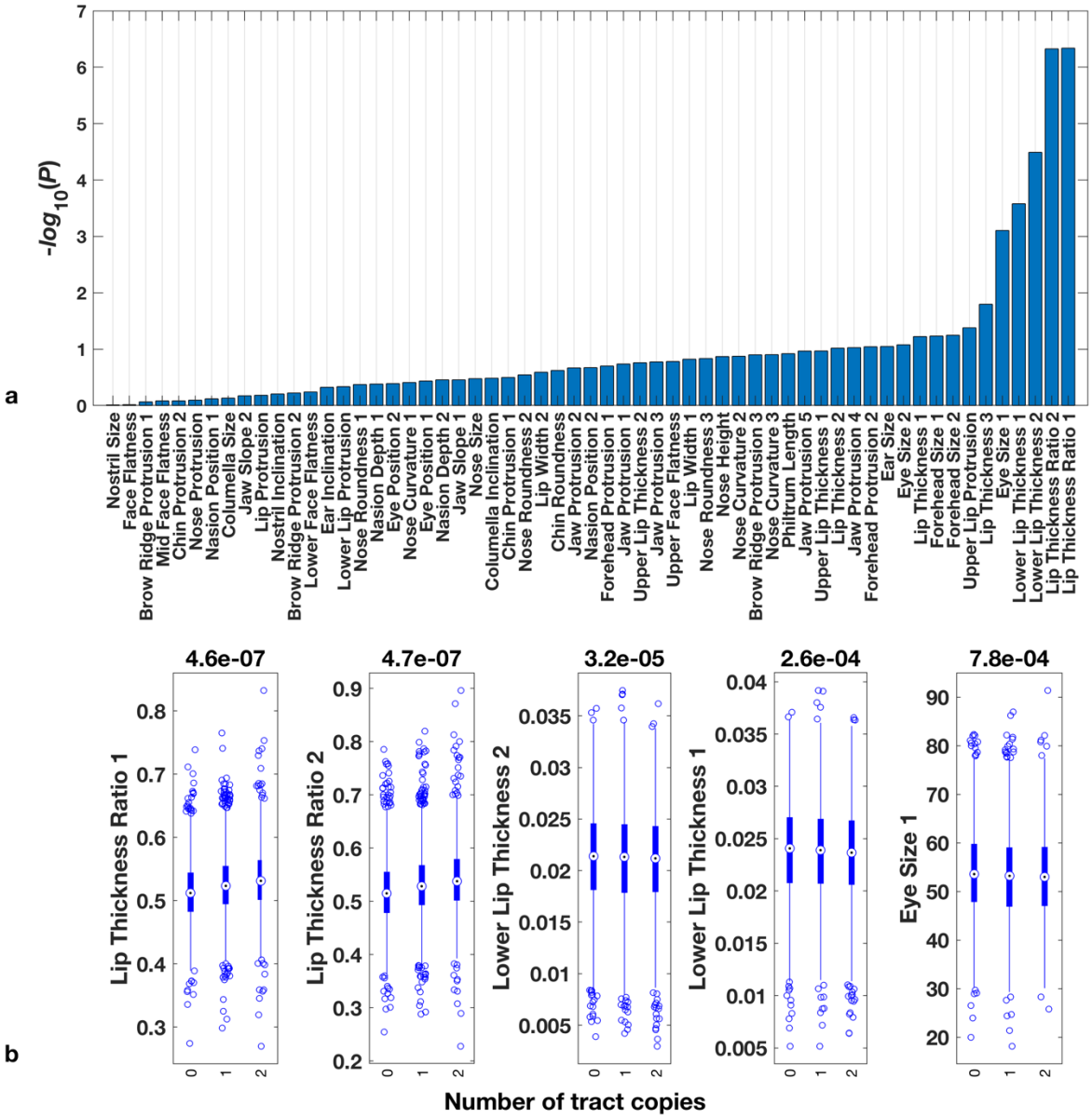

The 59 traits are ordered by their association *p*-values with the number of copies of the introgression tract in a linear regression including sex, age, BMI, landmarking operator and 6 genetic PCS (a). For the five traits with strongest association, we show the distribution of phenotype per number of copies of the Denisovan haplotype (b). The values on top of the boxes are the association *p*-values in a linear regression of the phenotype on 11 covariates (the genotype, plus sex, age, BMI, landmarking operator and 6 genetic PCs).

Supplementary tables

Supplementary table S1: Definition of the 59 profile traits examined in the CANDELA sample

Measurements were obtained based on the profile Landmarks (L) and Semi-Landmarks (SL) shown in Supplementary Fig. S1.
Notation: a - (dash) indicates the straight line between two points; a ∠ indicates the angle between three points.

Trait name	Measurement description
Forehead protrusion 1	Slope of L1-L2.
Forehead protrusion 2	Maximum length of a perpendicular to L1-L2 passing through SL20-24
Forehead size 1	Length of L1-L2.
Forehead size 2	Length of the curve connecting L1 and L2 passing through SL20 to SL24.
Brow ridge protrusion 1	Distance to L2 on the perpendicular to L1-L3.
Brow ridge protrusion 2	∠L3 L2 SL22.
Eye size 1	∠L4 L6 L5.
Eye size 2	Length of L4-L5.
Nasion depth 1	∠ L2 L3 SL29.
Nasion depth 2	Distance to L3 on the perpendicular to L2-SL30.
Nasion position 1	Ratio L3'-L8/L2-L8 where L3' is the projection of L3 onto L2-L8.
Nasion position 2	Length of L3-L3' where L3' is the projection of L3 onto the midpoint of L4-L5.
Eye position 1	∠L4 L3' L3, where L3' is the projection of L3 on the midpoint of L4-L5.
Eye position 2	Ratio L2-L4L5/L2-L8, where L4L5 is the projection onto L2-L8 of the midpoint between L4-L5.
Nose height	Length of L3-L8.
Nose protrusion	Length of the projection of L7 onto L3-L8.
Nose size	Distance between L3 and L8 passing through L7 and SL26 to SL32.
Nose roundness 1	∠L3 L7 L8.
Nose roundness 2	∠SL30 L7 SL31.
Nose roundness 3	Ratio measurement 19/ measurement18.
Nose curvature 1	Maximum distance between L3-L7 and SL 26 to SL 30.
Nose curvature 2	Ratio measurement 21/L3-L7.
Nose curvature 3	Smallest of ∠SL26 27 28 or ∠SL27 28 29.
Columella inclination	Slope of L8-SL31.
Nostril inclination	Slope of L9-L10.
Nostril size	Length of L9-L10.
Columella size	Length of L8-L8', where L8' is the projection of L8 onto L9-L10.
Lip thickness 1	Length of L11-L14.

Lip thickness 2	∠L11 L13 L14.
Lip thickness 3	∠L11 L12 L14.
Upper lip thickness 1	Length of L11-L12.
Lower lip thickness 1	Length of L12-L14.
Upper lip thickness 2	Length of L11-L12', where L12' is the projection of L12 onto L11-L14.
Lower lip thickness 2	Length of L12'-L14, where L12' is the projection of L12 onto L11-L14.
Lip thickness ratio 1	Ratio measurement 31/ (measurement 31 + measurement 32).
Lip thickness ratio 2	Ratio measurement 33/ (measurement 33 + measurement 34).
Upper lip protrusion	Length of L11-L11', where L11' is the projection of L11 onto L8-SL35.
Lower lip protrusion	Length of L14-L14', where L14' is the projection of L14 onto L8-SL35.
Lip protrusion	Maximum of measurements 37 or 38
Lip width 1	Length of L13-L13', where L13' is the projection of L13 onto the midpoint of L11-L14.
Lip width 2	Length of L12-L13.
Philtrum length	Length of L8-L11.
Chin protrusion 1	Maximum distance between SL34, SL35 or SL36 and L14-SL37.
Chin protrusion 2	∠L14 SL35 SL37.
Ear size	Length of L18-L19.
Ear inclination	Slope of L18-L19.
Jaw protrusion 1	Length of L15-L15', where L15' is the projection of L15 onto L1-L16.
Jaw protrusion 2	Ratio of the length of measurement 47/length of L14-L14', where L14' is the projection of L14 onto L1-L16.
Jaw protrusion 3	∠L14 L15 L16.
Jaw protrusion 4	Horizontal distance between L15 and L19.
Jaw protrusion 5	Ratio measurement 50/horizontal distance between L14 and L19.
Jaw slope 1	Slope of L15-L16.
Chin roundness	Ratio ∠SL37 L15 SL38/∠SL35 L15 SL40.
Jaw slope 2	∠L15 L16 L17.
Upper face flatness	Maximum distance to SL20-L7 of L2, L3 or SL21 to SL30.
Face flatness	Maximum distance to SL20-L15 of L2, L3, L7, L8, L11, L12, L14 or SL21 to SL37.
Brow ride protrusion 3	Ratio of distances L2-L19/L3-L19.
Mid face flatness	Ratio of distances L8-L19/L3-L19.
Lower face flatness	Ratio of distances L15-19/L3-L19.

Supplementary table S2: Concordance correlation coefficients (CCC)

See supplementary_tables_2-6.xlsx, sheet ‘Table S2’.

Supplementary table S3: Narrow-sense heritabilities, genetic and phenotypic correlations

See supplementary_tables_2-6.xlsx, sheet ‘Table S3’.

Supplementary table S4: Covariate correlations and regional ancestry contrasts

See supplementary_tables_2-6.xlsx, sheet ‘Table S4’.

Supplementary table S5: GWAS results

See supplementary_tables_2-6.xlsx, sheet ‘Table S5’.

Supplementary table S6: Annotations description and color key for a ChromHMM model with 25 states

See supplementary_tables_2-6.xlsx, sheet ‘Table S6’.

REFERENCES AND NOTES

1. L. Paternoster, A. I. Zhurov, A. M. Toma, J. P. Kemp, B. St Pourcain, N. J. Timpson, G. McMahon, W. McArdle, S. M. Ring, G. D. Smith, S. Richmond, D. M. Evans, Genome-wide association study of three-dimensional facial morphology identifies a variant in *PAX3* associated with nasion position. *Am. J. Hum. Genet.* **90**, 478–485 (2012).
2. F. Liu, F. van der Lijn, C. Schurmann, G. Zhu, M. M. Chakravarty, P. G. Hysi, A. Wollstein, O. Lao, M. de Bruijne, M. A. Ikram, A. van der Lugt, F. Rivadeneira, A. G. Uitterlinden, A. Hofman, W. J. Niessen, G. Homuth, G. de Zubicaray, K. L. McMahon, P. M. Thompson, A. Daboul, R. Puls, K. Hegenscheid, L. Bevan, Z. Pausova, S. E. Medland, G. W. Montgomery, M. J. Wright, C. Wicking, S. Boehringer, T. D. Spector, T. Paus, N. G. Martin, R. Biffar, M. Kayser, A genome-wide association study identifies five loci influencing facial morphology in Europeans. *PLOS Genet.* **8**, e1002932 (2012).
3. J. B. Cole, M. Manyama, E. Kimwaga, J. Mathayo, J. R. Larson, D. K. Liberton, K. Lukowiak, T. M. Ferrara, S. L. Riccardi, M. Li, W. Mio, M. Prochazkova, T. Williams, H. Li, K. L. Jones, O. D. Klein, S. A. Santorico, B. Hallgrimsson, R. A. Spritz, Genomewide association study of African children identifies association of *SCHIP1* and *PDE8A* with facial size and shape. *PLOS Genet.* **12**, e1006174 (2016).
4. K. Adhikari, M. Fuentes-Guajardo, M. Quinto-Sánchez, J. Mendoza-Revilla, J. C. Chacón-Duque, V. Acuña-Alonzo, C. Jaramillo, W. Arias, R. B. Lozano, G. M. Pérez, J. Gómez-Valdés, H. Villamil-Ramírez, T. Hunemeier, V. Ramallo, C. C. S. de Cerqueira, M. Hurtado, V. Villegas, V. Granja, C. Gallo, G. Poletti, L. Schuler-Faccini, F. M. Salzano, M.-C. Bortolini, S. Canizales-Quinteros, M. Cheeseman, J. Rosique, G. Bedoya, F. Rothhammer, D. Headon, R. González-José, D. Balding, A. Ruiz-Linares, A genome-wide association scan implicates *DCHS2*, *RUNX2*, *GLI3*, *PAX1* and *EDAR* in human facial variation. *Nat. Commun.* **7**, 11616 (2016).
5. M. K. Lee, J. R. Shaffer, E. J. Leslie, E. Orlova, J. C. Carlson, E. Feingold, M. L. Marazita, S. M. Weinberg, Genome-wide association study of facial morphology reveals novel associations with *FREM1* and *PARK2*. *PLOS ONE* **12**, e0176566 (2017).
6. J. R. Shaffer, E. Orlova, M. K. Lee, E. J. Leslie, Z. D. Raffensperger, C. L. Heike, M. L. Cunningham, J. T. Hecht, C. H. Kau, N. L. Nidey, L. M. Moreno, G. L. Wehby, J. C. Murray, C. A. Laurie, C. C. Laurie, J. Cole, T. Ferrara, S. Santorico, O. Klein, W. Mio, E. Feingold, B.

Hallgrimsson, R. A. Spritz, M. L. Marazita, S. M. Weinberg, Genome-wide association study reveals multiple loci influencing normal human facial morphology. *PLOS Genet.* **12**, e1006149 (2016).

7. J. K. Pickrell, T. Berisa, J. Z. Liu, L. Segurel, J. Y. Tung, D. A. Hinds, Detection and interpretation of shared genetic influences on 42 human traits. *Nat. Genet.* **48**, 709–717 (2016).
8. D. J. M. Crouch, B. Winney, W. P. Koppen, W. J. Christmas, K. Hutnik, T. Day, D. Meena, A. Boumertit, P. Hysi, A. Nessa, T. D. Spector, J. Kittler, W. F. Bodmer, Genetics of the human face: Identification of large-effect single gene variants. *Proc. Natl. Acad. Sci. U.S.A.* **115**, E676–E685 (2018).
9. S. Cha, J. E. Lim, A. Y. Park, J.-H. Do, S. W. Lee, C. Shin, N. H. Cho, J.-O. Kang, J. M. Nam, J.-S. Kim, K.-M. Woo, S.-H. Lee, J. Y. Kim, B. Oh, Identification of five novel genetic loci related to facial morphology by genome-wide association studies. *BMC Genomics* **19**, 481 (2018).
10. P. Claes, J. Roosenboom, J. D. White, T. Swigut, D. Sero, J. Li, M. K. Lee, A. Zaidi, B. C. Mattern, C. Liebowitz, L. Pearson, T. Gonzalez, E. J. Leslie, J. C. Carlson, E. Orlova, P. Suetens, D. Vandermeulen, E. Feingold, M. L. Marazita, J. R. Shaffer, J. Wysocka, M. D. Shriver, S. M. Weinberg, Genome-wide mapping of global-to-local genetic effects on human facial shape. *Nat. Genet.* **50**, 414–423 (2018).
11. P. Claes, D. K. Liberton, K. Daniels, K. M. Rosana, E. E. Quillen, L. N. Pearson, B. McEvoy, M. Bauchet, A. A. Zaidi, W. Yao, H. Tang, G. S. Barsh, D. M. Absher, D. A. Puts, J. Rocha, S. Beleza, R. W. Pereira, G. Baynam, P. Suetens, D. Vandermeulen, J. K. Wagner, J. S. Boster, M. D. Shriver, Modeling 3D facial shape from DNA. *PLOS Genet.* **10**, e1004224 (2014).
12. K. Indencleef, J. Roosenboom, H. Hoskens, J. D. White, M. D. Shriver, S. Richmond, H. Peeters, E. Feingold, M. L. Marazita, J. R. Shaffer, S. M. Weinberg, G. Hens, P. Claes, Six NSCL/P loci show associations with normal-range craniofacial variation. *Front. Genet.* **9**, 502 (2018).
13. A. Ruiz-Linares, K. Adhikari, V. Acuña-Alonzo, M. Quinto-Sanchez, C. Jaramillo, W. Arias, M. Fuentes, M. Pizarro, P. Everardo, F. de Avila, J. Gómez-Valdes, P. León-Mimila, T. Hunemeier, V. Ramallo, C. C. S. de Cerqueira, M.-W. Burley, E. Konca, M. Z. de Oliveira, M. R. Veronez, M. Rubio-Codina, O. Attanasio, S. Gibbon, N. Ray, C. Gallo, G. Poletti, J. Rosique, L. Schuler-Faccini, F. M. Salzano, M.-C. Bortolini, S. Canizales-Quinteros, F. Rothhammer, G. Bedoya, D. Balding, R. Gonzalez-José, Admixture in Latin America: Geographic structure, phenotypic diversity and self-perception of ancestry based on 7,342 individuals. *PLOS Genet.* **10**, e1004572 (2014).

14. J.-C. Chacón-Duque, K. Adhikari, M. Fuentes-Guajardo, J. Mendoza-Revilla, V. Acuña-Alonzo, R. Barquera, M. Quinto-Sánchez, J. Gómez-Valdés, P. E. Martínez, H. Villamil-Ramírez, T. Hünemeier, V. Ramallo, C. C. S. de Cerqueira, M. Hurtado, V. Villegas, V. Granja, M. Villena, R. Vásquez, E. Llop, J. R. Sandoval, A. A. Salazar-Granara, M.-L. Parolin, K. Sandoval, R. I. Peñaloza-Espinosa, H. Rangel-Villalobos, C. A. Winkler, W. Klitz, C. Bravi, J. Molina, D. Corach, R. Barrantes, V. Gomes, C. Resende, L. Gusmão, A. Amorim, Y. Xue, J.-M. Dugoujon, P. Moral, R. González-José, L. Schuler-Faccini, F. M. Salzano, M.-C. Bortolini, S. Canizales-Quinteros, G. Poletti, C. Gallo, G. Bedoya, F. Rothhammer, D. Balding, G. Hellenthal, A. Ruiz-Linares, Latin Americans show wide-spread Converso ancestry and imprint of local Native ancestry on physical appearance. *Nat. Commun.* **9**, 5388 (2018).
15. K. Adhikari, G. Reales, A. J. P. Smith, E. Konka, J. Palmen, M. Quinto-Sanchez, V. Acuña-Alonzo, C. Jaramillo, W. Arias, M. Fuentes, M. Pizarro, R. B. Lozano, G. M. Pérez, J. Gómez-Valdés, H. Villamil-Ramírez, T. Hunemeier, V. Ramallo, C. C. S. de Cerqueira, M. Hurtado, V. Villegas, V. Granja, C. Gallo, G. Poletti, L. Schuler-Faccini, F. M. Salzano, M.-C. Bortolini, S. Canizales-Quinteros, F. Rothhammer, G. Bedoya, R. Calderón, J. Rosique, M. Cheeseman, M. F. Bhutta, S. E. Humphries, R. Gonzalez-José, D. Headon, D. Balding, A. Ruiz-Linares, A genome-wide association study identifies multiple loci for variation in human ear morphology. *Nat. Commun.* **6**, 7500 (2015).
16. K. Adhikari, T. Fontanil, S. Cal, J. Mendoza-Revilla, M. Fuentes-Guajardo, J.-C. Chacón-Duque, F. Al-Saadi, J. A. Johansson, M. Quinto-Sanchez, V. Acuña-Alonzo, C. Jaramillo, W. Arias, R. B. Lozano, G. M. Perez, J. Gómez-Valdes, H. Villamil-Ramirez, T. Hunemeier, V. Ramallo, C. C. S. de Cerqueira, M. Hurtado, V. Villegas, V. Granja, C. Gallo, G. Poletti, L. Schuler-Faccini, F. M. Salzano, M.-C. Bortolini, S. Canizales-Quinteros, F. Rothhammer, G. Bedoya, R. Gonzalez-José, D. Headon, C. López-Otín, D. J. Tobin, D. Balding, A. Ruiz-Linares, A genome-wide association scan in admixed Latin Americans identifies loci influencing facial and scalp hair features. *Nat. Commun.* **7**, 10815 (2016).
17. K. Adhikari, J. Mendoza-Revilla, A. Sohail, M. Fuentes-Guajardo, J. Lampert, J. C. Chacón-Duque, M. Hurtado, V. Villegas, V. Granja, V. Acuña-Alonzo, C. Jaramillo, W. Arias, R. B. Lozano, P. Everardo, J. Gómez-Valdés, H. Villamil-Ramírez, C. C. S. de Cerqueira, T. Hunemeier, V. Ramallo, L. Schuler-Faccini, F. M. Salzano, R. Gonzalez-José, M.-C. Bortolini, S. Canizales-Quinteros, C. Gallo, G. Poletti, G. Bedoya, F. Rothhammer, D. J. Tobin, M. Fumagalli, D. Balding, A. Ruiz-

Linares, A GWAS in Latin Americans highlights the convergent evolution of lighter skin pigmentation in Eurasia. *Nat. Commun.* **10**, 358 (2019).

18. Z. Xiong, G. Dankova, L. J. Howe, M. K. Lee, P. G. Hysi, M. A. de Jong, G. Zhu, K. Adhikari, D. Li, Y. Li, B. Pan, E. Feingold, M. L. Marazita, J. R. Shaffer, K. M. Aloney, S.-H. Xu, L. Jin, S. Wang, F. M. S. de Vrij, B. Lendemeijer, S. Richmond, A. Zhurov, S. Lewis, G. C. Sharp, L. Paternoster, H. Thompson, R. Gonzalez-Jose, M. C. Bortolini, S. Canizales-Quinteros, C. Gallo, G. Poletti, G. Bedoya, F. Rothhammer, A. G. Uitterlinden, M. A. Ikram, E. Wolvius, S. A. Kushner, T. E. C. Nijsten, R.-J. T. S. Palstra, S. Boehringer, S. E. Medland, K. Tang, A. Ruiz-Linares, N. G. Martin, T. D. Spector, E. Stergiakouli, S. M. Weinberg, F. Liu, M. Kayser; On behalf of the International Visible Trait Genetics (VisiGen), Novel genetic loci affecting facial shape variation in humans. *eLife* **8**, e49898 (2019).
19. K. Usui, M. Tokita, Creating diversity in mammalian facial morphology: A review of potential developmental mechanisms. *Evodevo* **9**, 15 (2018).
20. R. S. Lacruz, C. B. Stringer, W. H. Kimbel, B. Wood, K. Harvati, P. O'Higgins, T. G. Bromage, J.-L. Arsuaga, The evolutionary history of the human face. *Nat. Ecol. Evol.* **3**, 726–736 (2019).
21. N. Davidenko, Silhouetted face profiles: A new methodology for face perception research. *J. Vis.* **7**, 6 (2007).
22. D. Speed, N. Cai; UCLEB Consortium, M. R. Johnson, S. Nejentsev, D. J. Balding, Reevaluation of SNP heritability in complex human traits. *Nat. Genet.* **49**, 986–992 (2017).
23. 1000 Genomes Project Consortium, A. Auton, L. D. Brooks, R. M. Durbin, E. P. Garrison, H. M. Kang, J. O. Korbel, J. L. Marchini, S. McCarthy, G. A. McVean, G. R. Abecasis, A global reference for human genetic variation. *Nature* **526**, 68–74 (2015).
24. C. C. Chang, C. C. Chow, L. C. Tellier, S. Vattikuti, S. M. Purcell, J. J. Lee, Second-generation PLINK: Rising to the challenge of larger and richer datasets. *Gigascience* **4**, 7 (2015).
25. Y. Benjamini, Y. Hochberg, Controlling the false discovery rate: A practical and powerful approach to multiple testing. *J. Roy. Statist. Soc. Ser. B* **57**, 289–300 (1995).
26. S. Birnbaum, K. U. Ludwig, H. Reutter, S. Herms, M. Steffens, M. Rubini, C. Baluardo, M. Ferrian, N. A. de Assis, M. A. Alblas, S. Barth, J. Freudenberg, C. Lauster, G. Schmidt, M. Scheer, B. Braumann, S. J. Bergé, R. H. Reich, F. Schiefke, A. Hemprich, S. Pötzsch, R. P. Steegers-Theunissen, B. Pötzsch, S. Moebus, B. Horsthemke, F.-J. Kramer, T. F. Wienker, P. A. Mossey, P. Propping, S. Cichon, P. Hoffmann, M. Knapp, M. M. Nöthen, E. Mangold, Key susceptibility locus

for nonsyndromic cleft lip with or without cleft palate on chromosome 8q24. *Nat. Genet.* **41**, 473–477 (2009).

27. A. Wilderman, J. VanOudenhove, J. Kron, J. P. Noonan, J. Cotney, High-resolution epigenomic atlas of human embryonic craniofacial development. *Cell Rep.* **23**, 1581–1597 (2018).
28. E. M. Schmidt, J. Zhang, W. Zhou, J. Chen, K. L. Mohlke, Y. E. Chen, C. J. Willer, GREGOR: Evaluating global enrichment of trait-associated variants in epigenomic features using a systematic, data-driven approach. *Bioinformatics* **31**, 2601–2606 (2015).
29. I. M. Heid, A. U. Jackson, J. C. Randall, T. W. Winkler, L. Qi, V. Steinthorsdottir, G. Thorleifsson, M. C. Zillikens, E. K. Speliotes, R. Mägi, T. Workalemahu, C. C. White, N. Bouatia-Naji, T. B. Harris, S. I. Berndt, E. Ingelsson, C. J. Willer, M. N. Weedon, J. Luan, S. Vedantam, T. Esko, T. O. Kilpeläinen, Z. Kutalik, S. Li, K. L. Monda, A. L. Dixon, C. C. Holmes, L. M. Kaplan, L. Liang, J. L. Min, M. F. Moffatt, C. Molony, G. Nicholson, E. E. Schadt, K. T. Zondervan, M. F. Feitosa, T. Ferreira, H. L. Allen, R. J. Weyant, E. Wheeler, A. R. Wood; MAGIC, K. Estrada, M. E. Goddard, G. Lettre, M. Mangino, D. R. Nyholt, S. Purcell, A. V. Smith, P. M. Visscher, J. Yang, S. A. Mc Carroll, J. Nemesh, B. F. Voight, D. Absher, N. Amin, T. Aspelund, L. Coin, N. L. Glazer, C. Hayward, N. L. Heard-Costa, J.-J. Hottenga, A. Johansson, T. Johnson, M. Kaakinen, K. Kapur, S. Ketkar, J. W. Knowles, P. Kraft, A. T. Kraja, C. Lamina, M. F. Leitzmann, B. Mc Knight, A. P. Morris, K. K. Ong, J. R. B. Perry, M. J. Peters, O. Polasek, I. Prokopenko, N. W. Rayner, S. Ripatti, F. Rivadeneira, N. R. Robertson, S. Sanna, U. Sovio, I. Surakka, A. Teumer, S. van Wingerden, V. Vitart, J. H. Zhao, C. Cavalcanti-Proença, P. S. Chines, E. Fisher, J. R. Kulzer, C. Lecoeur, N. Narisu, C. Sandholt, L. J. Scott, K. Silander, K. Stark, M.-L. Tammesoo, T. M. Teslovich, N. J. Timpson, R. M. Watanabe, R. Welch, D. I. Chasman, M. N. Cooper, J.-O. Jansson, J. Kettunen, R. W. Lawrence, N. Pellikka, M. Perola, L. Vandenput, H. Alavere, P. Almgren, L. D. Atwood, A. J. Bennett, R. Biffar, L. L. Bonnycastle, S. R. Bornstein, T. A. Buchanan, H. Campbell, I. N. M. Day, M. Dei, M. Dörr, P. Elliott, M. R. Erdos, J. G. Eriksson, N. B. Freimer, M. Fu, S. Gaget, E. J. C. Geus, A. P. Gjesing, H. Grallert, J. Grässler, C. J. Groves, C. Guiducci, A.-L. Hartikainen, N. Hassanali, A. S. Havulinna, K.-H. Herzig, A. A. Hicks, J. Hui, W. Igl, P. Jousilahti, A. Jula, E. Kajantie, L. Kinnunen, I. Kolcic, S. Koskinen, P. Kovacs, H. K. Kroemer, V. Krzelj, J. Kuusisto, K. Kvaloy, J. Laitinen, O. Lantieri, G. M. Lathrop, M.-L. Lokki, R. N. Luben, B. Ludwig, W. L. Mc Ardle, A. Mc Carthy, M. A. Morken, M. Nelis, M. J. Neville, G. Paré, A. N. Parker, J. F. Peden, I. Pichler, K. H. Pietiläinen, C. G. P. Platou, A. Pouta, M. Ridderstråle, N. J. Samani, J. Saramies, J.

Sinisalo, J. H. Smit, R. J. Strawbridge, H. M. Stringham, A. J. Swift, M. Teder-Laving, B. Thomson, G. Usala, J. B. J. van Meurs, G.-J. van Ommen, V. Vatin, C. B. Volpato, H. Wallaschofski, G. B. Walters, E. Widen, S. H. Wild, G. Willemsen, D. R. Witte, L. Zgaga, P. Zitting, J. P. Beilby, A. L. James, M. Kähönen, T. Lehtimäki, M. S. Nieminen, C. Ohlsson, L. J. Palmer, O. Raitakari, P. M. Ridker, M. Stumvoll, A. Tönjes, J. Viikari, B. Balkau, Y. Ben-Shlomo, R. N. Bergman, H. Boeing, G. D. Smith, S. Ebrahim, P. Froguel, T. Hansen, C. Hengstenberg, K. Hveem, B. Isomaa, T. Jørgensen, F. Karpe, K.-T. Khaw, M. Laakso, D. A. Lawlor, M. Marre, T. Meitinger, A. Metspalu, K. Midthjell, O. Pedersen, V. Salomaa, P. E. H. Schwarz, T. Tuomi, J. Tuomilehto, T. T. Valle, N. J. Wareham, A. M. Arnold, J. S. Beckmann, S. Bergmann, E. Boerwinkle, D. I. Boomsma, M. J. Caulfield, F. S. Collins, G. Eiriksdottir, V. Gudnason, U. Gyllensten, A. Hamsten, A. T. Hattersley, A. Hofman, F. B. Hu, T. Illig, C. Iribarren, M.-R. Jarvelin, W. H. L. Kao, J. Kaprio, L. J. Launer, P. B. Munroe, B. Oostra, B. W. Penninx, P. P. Pramstaller, B. M. Psaty, T. Quertermous, A. Rissanen, I. Rudan, A. R. Shuldiner, N. Soranzo, T. D. Spector, A.-C. Syvanen, M. Uda, A. Uitterlinden, H. Völzke, P. Vollenweider, J. F. Wilson, J. C. Witteman, A. F. Wright, G. R. Abecasis, M. Boehnke, I. B. Borecki, P. Deloukas, T. M. Frayling, L. C. Groop, T. Haritunians, D. J. Hunter, R. C. Kaplan, K. E. North, J. R. O'Connell, L. Peltonen, D. Schlessinger, D. P. Strachan, J. N. Hirschhorn, T. L. Assimes, H.-E. Wichmann, U. Thorsteinsdottir, C. M. van Duijn, K. Stefansson, L. A. Cupples, R. J. F. Loos, I. Barroso, M. I. Mc Carthy, C. S. Fox, K. L. Mohlke, C. M. Lindgren, Meta-analysis identifies 13 new loci associated with waist-hip ratio and reveals sexual dimorphism in the genetic basis of fat distribution. *Nat. Genet.* **42**, 949–960 (2010).

30. M. Fumagalli, I. Moltke, N. Grarup, F. Racimo, P. Bjerregaard, M. E. Jorgensen, T. S. Korneliussen, P. Gerbault, L. Skotte, A. Linneberg, C. Christensen, I. Brandslund, T. Jorgensen, E. Huerta-Sanchez, E. B. Schmidt, O. Pedersen, T. Hansen, A. Albrechtsen, R. Nielsen, Greenlandic Inuit show genetic signatures of diet and climate adaptation. *Science* **349**, 1343–1347 (2015).
31. F. Racimo, D. Gokhman, M. Fumagalli, A. Ko, T. Hansen, I. Moltke, A. Albrechtsen, L. Carmel, E. Huerta-Sanchez, R. Nielsen, Archaic adaptive introgression in TBX15/WARS2. *Mol. Biol. Evol.* **34**, 509–524 (2017).
32. S. Sankararaman, S. Mallick, N. Patterson, D. Reich, The combined landscape of denisovan and Neanderthal ancestry in present-day humans. *Curr. Biol.* **26**, 1241–1247 (2016).

33. H. Kim, N. Takegahara, M. C. Walsh, S. A. Middleton, J. Yu, J. Shirakawa, J. Ueda, Y. Fujihara, M. Ikawa, M. Ishii, J. Kim, Y. Choi, IgSF11 regulates osteoclast differentiation through association with the scaffold protein PSD-95. *Bone Res.* **8**, 5 (2020).
34. N. Hirsch, R. Eshel, R. B. Yaacov, T. Shahar, F. Shmulevich, I. Dahan, N. Levaot, T. Kaplan, D. G. Lupianez, R. Y. Birnbaum, Unraveling the transcriptional regulation of TWIST1 in limb development. *PLOS Genet.* **14**, e1007738 (2018).
35. G. Kichaev, G. Bhatia, P. R. Loh, S. Gazal, K. Burch, M. K. Freund, A. Schoech, B. Pasaniuc, A. L. Price, Leveraging polygenic functional enrichment to improve GWAS power. *Am. J. Hum. Genet.* **104**, 65–75 (2019).
36. C. Medina-Gomez, J. P. Kemp, K. Trajanoska, J. Luan, A. Chesi, T. S. Ahluwalia, D. O. Mook-Kanamori, A. Ham, F. P. Hartwig, D. S. Evans, R. Joro, I. Nedeljkovic, H.-F. Zheng, K. Zhu, M. Atalay, C.-T. Liu, M. Nethander, L. Broer, G. Porleifsson, B. H. Mullin, S. K. Handelman, M. A. Nalls, L. E. Jessen, D. H. M. Heppe, J. B. Richards, C. Wang, B. Chawes, K. E. Schraut, N. Amin, N. Wareham, D. Karasik, N. Van der Velde, M. A. Ikram, B. S. Zemel, Y. Zhou, C. J. Carlsson, Y. Liu, F. E. McGuigan, C. G. Boer, K. Bønnelykke, S. H. Ralston, J. A. Robbins, J. P. Walsh, M. C. Zillikens, C. Langenberg, R. Li-Gao, F. M. K. Williams, T. B. Harris, K. Akesson, R. D. Jackson, G. Sigurdsson, M. den Heijer, B. C. J. van der Eerden, J. van de Peppel, T. D. Spector, C. Pennell, B. L. Horta, J. F. Felix, J. H. Zhao, S. G. Wilson, R. de Mutsert, H. Bisgaard, U. Styrkársdóttir, V. W. Jaddoe, E. Orwoll, T. A. Lakka, R. Scott, S. F. A. Grant, M. Lorentzon, C. M. van Duijn, J. F. Wilson, K. Stefansson, B. M. Psaty, D. P. Kiel, C. Ohlsson, E. Ntzani, A. J. van Wijnen, V. Forgetta, M. Ghanbari, J. G. Logan, G. R. Williams, J. H. D. Bassett, P. I. Croucher, E. Evangelou, A. G. Uitterlinden, C. L. Ackert-Bicknell, J. H. Tobias, D. M. Evans, F. Rivadeneira, Life-course genome-wide association study meta-analysis of total body BMD and assessment of age-specific effects. *Am. J. Hum. Genet.* **102**, 88–102 (2018).
37. K. Reynolds, P. Kumari, L. S. Rincon, R. Gu, Y. Ji, S. Kumar, C. J. Zhou, Wnt signaling in orofacial clefts: Crosstalk, pathogenesis and models. *Dis. Model. Mech.* **12**, dmm037051 (2019).
38. R. Da Costa, M. Bordessoules, M. Guilleman, V. Carmignac, V. Lhussiez, H. Courot, A. Bataille, A. Chlémaire, C. Bruno, P. Fauque, C. Thauvin, L. Faivre, L. Duplomb, Vps13b is required for acrosome biogenesis through functions in Golgi dynamic and membrane trafficking. *Cell. Mol. Life Sci.* **77**, 511–529 (2019).

39. L. F. Pallares, P. Carbonetto, S. Gopalakrishnan, C. C. Parker, C. L. Ackert-Bicknell, A. A. Palmer, D. Tautz, Mapping of craniofacial traits in outbred mice identifies major developmental genes involved in shape determination. *PLOS Genet.* **11**, e1005607 (2015).
40. R. Soldatov, M. Kaucka, M. E. Kastriti, J. Petersen, T. Chontorotzea, L. Englmaier, N. Akkuratova, Y. Yang, M. Häring, V. Dyachuk, C. Bock, M. Farlik, M. L. Piacentino, F. Boismoreau, M. M. Hilscher, C. Yokota, X. Y. Qian, M. Nilsson, M. E. Bronner, L. Croci, W.-Y. Hsiao, D. A. Guertin, J.-F. Brunet, G. G. Consalez, P. Ernfors, K. Fried, P. V. Kharchenko, I. Adameyko, Spatiotemporal structure of cell fate decisions in murine neural crest. *Science* **364**, eaas9536 (2019).
41. S. L. Prescott, R. Srinivasan, M. C. Marchetto, I. Grishina, I. Narvaiza, L. Selleri, F. H. Gage, T. Swigut, J. Wysocka, Enhancer divergence and cis-regulatory evolution in the human and chimp neural crest. *Cell* **163**, 68–83 (2015).
42. J. Hu, M. P. Verzi, A. S. Robinson, P. L.-F. Tang, L. L. Hua, S.-M. Xu, P.-Y. Kwok, B. L. Black, Endothelin signaling activates Mef2c expression in the neural crest through a MEF2C-dependent positive-feedback transcriptional pathway. *Development* **142**, 2775–2780 (2015).
43. M. Dannemann, F. Racimo, Something old, something borrowed: Admixture and adaptation in human evolution. *Curr. Opin. Genet. Dev.* **53**, 1–8 (2018).
44. W. A. Whyte, D. A. Orlando, D. Hnisz, B. J. Abraham, C. Y. Lin, M. H. Kagey, P. B. Rahl, T. I. Lee, R. A. Young, Master transcription factors and mediator establish super-enhancers at key cell identity genes. *Cell* **153**, 307–319 (2013).
45. M. Segura-Puimedon, I. Sahun, E. Velot, P. Dubus, C. Borralleras, A. J. Rodrigues, M. C. Valero, O. Valverde, N. Sousa, Y. Herault, M. Dierssen, L. A. Perez-Jurado, V. Campuzano, Heterozygous deletion of the Williams-Beuren syndrome critical interval in mice recapitulates most features of the human disorder. *Hum. Mol. Genet.* **23**, 6481–6494 (2014).
46. W. Seifert, J. Kuhnisch, T. Maritzen, S. Lommatzsch, H. C. Hennies, S. Bachmann, D. Horn, V. Haucke, Cohen syndrome-associated protein COH1 physically and functionally interacts with the small GTPase RAB6 at the Golgi complex and directs neurite outgrowth. *J. Biol. Chem.* **290**, 3349–3358 (2015).
47. L. Duplomb, S. Duvet, D. Picot, G. Jego, S. El Chehadeh-Djebbar, N. Marle, N. Gigot, B. Aral, V. Carmignac, J. Thevenon, E. Lopez, J. B. Riviere, A. Klein, C. Philippe, N. Droin, E. Blair, F. Girodon, J. Donadieu, C. Bellanne-Chantelot, L. Delva, J. C. Michalski, E. Solary, L. Faivre, F.

Foulquier, C. Thauvin-Robinet, Cohen syndrome is associated with major glycosylation defects. *Hum. Mol. Genet.* **23**, 2391–2399 (2014).

48. R. Peanne, P. de Lonlay, F. Foulquier, U. Kornak, D. J. Lefeber, E. Morava, B. Perez, N. Seta, C. Thiel, E. Van Schaftingen, G. Matthijs, J. Jaeken, Congenital disorders of glycosylation (CDG): Quo vadis? *Eur. J. Med. Genet.* **61**, 643–663 (2018).
49. A. Vaysse, A. Ratnakumar, T. Derrien, E. Axelsson, G. R. Pielberg, S. Sigurdsson, T. Fall, E. H. Seppälä, M. S. T. Hansen, C. T. Lawley, E. K. Karlsson; LUPA Consortium, D. Bannasch, C. Vilà, H. Lohi, F. Galibert, M. Fredholm, J. Häggström, A. Hedhammar, C. André, K. Lindblad-Toh, C. Hitte, M. T. Webster, Identification of genomic regions associated with phenotypic variation between dog breeds using selection mapping. *PLOS Genet.* **7**, e1002316 (2011).
50. R. E. Green, J. Krause, A. W. Briggs, T. Maricic, U. Stenzel, M. Kircher, N. Patterson, H. Li, W. Zhai, M. H.-Y. Fritz, N. F. Hansen, E. Y. Durand, A.-S. Malaspinas, J. D. Jensen, T. Marques-Bonet, C. Alkan, K. Prüfer, M. Meyer, H. A. Burbano, J. M. Good, R. Schultz, A. Aximu-Petri, A. Butthof, B. Höber, B. Höffner, M. Siegemund, A. Weihmann, C. Nusbaum, E. S. Lander, C. Russ, N. Novod, J. Affourtit, M. Egholm, C. Verna, P. Rudan, D. Brajkovic, Ž. Kucan, I. Gušic, V. B. Doronichev, L. V. Golovanova, C. Lalueza-Fox, M. de la Rasilla, J. Fortea, A. Rosas, R. W. Schmitz, P. L. F. Johnson, E. E. Eichler, D. Falush, E. Birney, J. C. Mullikin, M. Slatkin, R. Nielsen, J. Kelso, M. Lachmann, D. Reich, S. Pääbo, A draft sequence of the Neandertal genome. *Science* **328**, 710–722 (2010).
51. K. E. Sears, A. Goswami, J. J. Flynn, L. A. Niswander, The correlated evolution of Runx2 tandem repeats, transcriptional activity, and facial length in carnivora. *Evol. Dev.* **9**, 555–565 (2007).
52. T. B. Ritzman, N. Banovich, K. P. Buss, J. Guida, M. A. Rubel, J. Pinney, B. Khang, M. J. Ravosa, A. C. Stone, Facing the facts: The Runx2 gene is associated with variation in facial morphology in primates. *J. Hum. Evol.* **111**, 139–151 (2017).
53. J. Caple, C. N. Stephan, A standardized nomenclature for craniofacial and facial anthropometry. *Int. J. Leg. Med.* **130**, 863–879 (2016).
54. F. J. Rohlf, The tps series of software. *Hystrix It. J. Mamm.* **26**, 9–12 (2015).
55. C. P. Klingenberg, MorphoJ: An integrated software package for geometric morphometrics. *Mol. Ecol. Resour.* **11**, 353–357 (2011).

56. S. Ritz-Timme, P. Gabriel, J. Tutkuviene, P. Poppa, Z. Obertová, D. Gibelli, D. De Angelis, M. Ratnayake, R. Rizgeliene, A. Barkus, C. Cattaneo, Metric and morphological assessment of facial features: A study on three European populations. *Forensic Sci. Int.* **207**, 239.e1–238 (2011).
57. L. G. Farkas, M. J. Katic, C. R. Forrest, Comparison of craniofacial measurements of young adult African-American and North American white males and females. *Ann. Plast. Surg.* **59**, 692–698 (2007).
58. L. I. Lin, A concordance correlation coefficient to evaluate reproducibility. *Biometrics* **45**, 255–268 (1989).
59. J. O'Connell, D. Gurdasani, O. Delaneau, N. Pirastu, S. Ulivi, M. Cocca, M. Traglia, J. Huang, J. E. Huffman, I. Rudan, R. McQuillan, R. M. Fraser, H. Campbell, O. Polasek, G. Asiki, K. Ekoru, C. Hayward, A. F. Wright, V. Vitart, P. Navarro, J. F. Zagury, J. F. Wilson, D. Toniolo, P. Gasparini, N. Soranzo, M. S. Sandhu, J. Marchini, A general approach for haplotype phasing across the full spectrum of relatedness. *PLOS Genet.* **10**, e1004234 (2014).
60. B. Howie, C. Fuchsberger, M. Stephens, J. Marchini, G. R. Abecasis, Fast and accurate genotype imputation in genome-wide association studies through pre-phasing. *Nat. Genet.* **44**, 955–959 (2012).
61. D. H. Alexander, J. Novembre, K. Lange, Fast model-based estimation of ancestry in unrelated individuals. *Genome Res.* **19**, 1655–1664 (2009).
62. J. Yang, S. H. Lee, M. E. Goddard, P. M. Visscher, GCTA: A tool for genome-wide complex trait analysis. *Am. J. Hum. Genet.* **88**, 76–82 (2011).
63. C. P. Klingenberg, M. Barluenga, A. Meyer, Shape analysis of symmetric structures: Quantifying variation among individuals and asymmetry. *Evolution* **56**, 1909–1920 (2002).
64. C. R. Goodall, Procrustes methods in the statistical analysis of shape (with discussion and rejoinder). *J. Roy. Stat. Soc. Ser. B* **53** 285–339 (1991).
65. H. M. Kang, J. H. Sul, S. K. Service, N. A. Zaitlen, S.-Y. Kong, N. B. Freimer, C. Sabatti, E. Eskin, Variance component model to account for sample structure in genome-wide association studies. *Nat. Genet.* **42**, 348–354 (2010).
66. J. Nicod, R. W. Davies, N. Cai, C. Hassett, L. Goodstadt, C. Cosgrove, B. K. Yee, V. Lionikaite, R. E. MC Intyre, C. A. Remme, E. M. Lodder, J. S. Gregory, T. Hough, R. Joynson, H. Phelps, B. Nell, C. Rowe, J. Wood, A. Walling, N. Bopp, A. Bhomra, P. Hernandez-Pliego, J. Callebert, R. M. Aspden, N. P. Talbot, P. A. Robbins, M. Harrison, M. Fray, J.-M. Launay, Y. M. Pinto, D. A.

Blizard, C. R. Bezzina, D. J. Adams, P. Franken, T. Weaver, S. Wells, S. D. M. Brown, P. K. Potter, P. Klenerman, A. Lionikas, R. Mott, J. Flint, Genome-wide association of multiple complex traits in outbred mice by ultra-low-coverage sequencing. *Nat. Genet.* **48**, 912–918 (2016).

67. Roadmap Epigenomics Consortium, A. Kundaje, W. Meuleman, J. Ernst, M. Bilenky, A. Yen, A. Heravi-Moussavi, P. Kheradpour, Z. Zhang, J. Wang, M. J. Ziller, V. Amin, J. W. Whitaker, M. D. Schultz, L. D. Ward, A. Sarkar, G. Quon, R. S. Sandstrom, M. L. Eaton, Y.-C. Wu, A. R. Pfenning, X. Wang, M. Claussnitzer, Y. Liu, C. Coarfa, R. Alan Harris, N. Shoresh, C. B. Epstein, E. Gjoneska, D. Leung, W. Xie, R. David Hawkins, R. Lister, C. Hong, P. Gascard, A. J. Mungall, R. Moore, E. Chuah, A. Tam, T. K. Canfield, R. Scott Hansen, R. Kaul, P. J. Sabo, M. S. Bansal, A. Carles, J. R. Dixon, K.-H. Farh, S. Feizi, R. Karlic, A.-R. Kim, A. Kulkarni, D. Li, R. Lowdon, G. N. Elliott, T. R. Mercer, S. J. Neph, V. Onuchic, P. Polak, N. Rajagopal, P. Ray, R. C. Sallari, K. T. Siebenthall, N. A. Sinnott-Armstrong, M. Stevens, R. E. Thurman, J. Wu, B. Zhang, X. Zhou, A. E. Beaudet, L. A. Boyer, P. L. De Jager, P. J. Farnham, S. J. Fisher, D. Haussler, S. J. M. Jones, W. Li, M. A. Marra, M. T. Mc Manus, S. Sunyaev, J. A. Thomson, T. D. Tlsty, L.-H. Tsai, W. Wang, R. A. Waterland, M. Q. Zhang, L. H. Chadwick, B. E. Bernstein, J. F. Costello, J. R. Ecker, M. Hirst, A. Meissner, A. Milosavljevic, B. Ren, J. A. Stamatoyannopoulos, T. Wang, M. Kellis, Integrative analysis of 111 reference human epigenomes. *Nature* **518**, 317–330 (2015).
68. X. Yi, Y. Liang, E. Huerta-Sanchez, X. Jin, Z. X. P. Cuo, J. E. Pool, X. Xu, H. Jiang, N. Vinckenbosch, T. S. Korneliussen, H. Zheng, T. Liu, W. He, K. Li, R. Luo, X. Nie, H. Wu, M. Zhao, H. Cao, J. Zou, Y. Shan, S. Li, Q. Yang, Asan, P. Ni, G. Tian, J. Xu, X. Liu, T. Jiang, R. Wu, G. Zhou, M. Tang, J. Qin, T. Wang, S. Feng, G. Li, Huasang, J. Luosang, W. Wang, F. Chen, Y. Wang, X. Zheng, Z. Li, Z. Bianba, G. Yang, X. Wang, S. Tang, G. Gao, Y. Chen, Z. Luo, L. Gusang, Z. Cao, Q. Zhang, W. Ouyang, X. Ren, H. Liang, H. Zheng, Y. Huang, J. Li, L. Bolund, K. Kristiansen, Y. Li, Y. Zhang, X. Zhang, R. Li, S. Li, H. Yang, R. Nielsen, J. Wang, J. Wang, Sequencing of 50 human exomes reveals adaptation to high altitude. *Science* **329**, 75–78 (2010).
69. B. K. Maples, S. Gravel, E. E. Kenny, C. D. Bustamante, RFMix: A discriminative modeling approach for rapid and robust local-ancestry inference. *Am. J. Hum. Genet.* **93**, 278–288 (2013).
70. S. Boehringer, F. van der Lijn, F. Liu, M. Gunther, S. Sinigerova, S. Nowak, K. U. Ludwig, R. Herberz, S. Klein, A. Hofman, A. G. Uitterlinden, W. J. Niessen, M. M. B. Breteler, A. van der Lugt, R. P. Wurtz, M. M. Nothen, B. Horsthemke, D. Wieczorek, E. Mangold, M. Kayser, Genetic

determination of human facial morphology: Links between cleft-lips and normal variation. *Eur. J. Hum. Genet.* **19**, 1192–1197 (2011).

71. K. U. Ludwig, A. C. Bohmer, J. Bowes, M. Nikolic, N. Ishorst, N. Wyatt, N. L. Hammond, L. Golz, F. Thieme, S. Barth, H. Schuenke, J. Klamt, M. Spielmann, K. Aldhorae, A. Rojas-Martinez, M. M. Nothen, A. Rada-Iglesias, M. J. Dixon, M. Knapp, E. Mangold, Imputation of orofacial clefting data identifies novel risk loci and sheds light on the genetic background of cleft lip ± cleft palate and cleft palate only. *Hum. Mol. Genet.* **26**, 829–842 (2017).
72. L. Qiao, Y. Yang, P. Fu, S. Hu, H. Zhou, S. Peng, J. Tan, Y. Lu, H. Lou, D. Lu, S. Wu, J. Guo, L. Jin, Y. Guan, S. Wang, S. Xu, K. Tang, Genome-wide variants of Eurasian facial shape differentiation and a prospective model of DNA based face prediction. *J. Genet. Genomics* **45**, 419–432 (2018).
73. T. H. Beaty, J. C. Murray, M. L. Marazita, R. G. Munger, I. Ruczinski, J. B. Hetmanski, K. Y. Liang, T. Wu, T. Murray, M. D. Fallin, R. A. Redett, G. Raymond, H. Schwender, S.-C. Jin, M. E. Cooper, M. Dunnwald, M. A. Mansilla, E. Leslie, S. Bullard, A. C. Lidral, L. M. Moreno, R. Menezes, A. R. Vieira, A. Petrin, A. J. Wilcox, R. T. Lie, E. W. Jabs, Y. H. Wu-Chou, P. K. Chen, H. Wang, X. Ye, S. Huang, V. Yeow, S. S. Chong, S. H. Jee, B. Shi, K. Christensen, M. Melbye, K. F. Doheny, E. W. Pugh, H. Ling, E. E. Castilla, A. E. Czeizel, L. Ma, L. L. Field, L. Brody, F. Pangilinan, J. L. Mills, A. M. Molloy, P. N. Kirke, J. M. Scott, M. Arcos-Burgos, A. F. Scott, A genome-wide association study of cleft lip with and without cleft palate identifies risk variants near MAFB and ABCA4. *Nat. Genet.* **42**, 525–529 (2010).
74. G. Fatemifar, C. J. Hoggart, L. Paternoster, J. P. Kemp, I. Prokopenko, M. Horikoshi, V. J. Wright, J. H. Tobias, S. Richmond, A. I. Zhurov, A. M. Toma, A. Pouta, A. Taanila, K. Sipila, R. Lähdesmäki, D. Pillas, F. Geller, B. Feenstra, M. Melbye, E. A. Nohr, S. M. Ring, B. S. Pourcain, N. J. Timpson, G. D. Smith, M.-R. Jarvelin, D. M. Evans, Genome-wide association study of primary tooth eruption identifies pleiotropic loci associated with height and craniofacial distances. *Hum. Mol. Genet.* **22**, 3807–3817 (2013).
75. S. Schuler, J. Hauptmann, B. Perner, M. M. Kessels, C. Englert, B. Qualmann, Ciliated sensory hair cell formation and function require the F-BAR protein syndapin I and the WH2 domain-based actin nucleator Cobl. *J. Cell Sci.* **126**, 196–208 (2013).
76. S. C. Goetz, K. V. Anderson, The primary cilium: A signalling centre during vertebrate development. *Nat. Rev. Genet.* **11**, 331–344 (2010).

77. X. Zhu, F. Wang, Y. Zhao, P. Yang, J. Chen, H. Sun, L. Liu, W. Li, L. Pan, Y. Guo, Z. Kou, Y. Zhang, C. Zhou, J. He, X. Zhang, J. Li, W. Han, J. Li, G. Liu, S. Gao, Z. Yang, A gain-of-function mutation in *Tnni2* impeded bone development through increasing *Hif3a* expression in DA2B mice. *PLOS Genet.* **10**, e1004589 (2014).
78. B. Wei, J.-P. Jin, *TNNT1*, *TNNT2*, and *TNNT3*: Isoform genes, regulation, and structure-function relationships. *Gene* **582**, 1–13 (2016).
79. S. Yakar, H. Werner, C. J. Rosen, Insulin-like growth factors: Actions on the skeleton. *J. Mol. Endocrinol.* **61**, T115–T137 (2018).
80. N. Wittkopp, E. Huntzinger, C. Weiler, J. Sauliere, S. Schmidt, M. Sonawane, E. Izaurralde, Nonsense-mediated mRNA decay effectors are essential for zebrafish embryonic development and survival. *Mol. Cell. Biol.* **29**, 3517–3528 (2009).